140

McDonald, Jeffrey

From:	Gilmore, Tyler J [Tyler.Gilmore@pnnl.gov]
Sent:	Friday, January 31, 2014 11:31 PM
To:	McDonald, Jeffrey
Cc:	Greenhagen, Andrew; Bayer, MaryRose
Subject:	Area of Review Delination and Maximum Well Pressure Calculations
Attachments:	EPA_IR7_for_FG-RPT-017-Final.pdf

Jeff,
Attached are our response to your questions about the delineation of the Area of Review and on our maximum well pressure calculations. (IR7_01-23-2014). Please call if you have any questions.
Thanks
Tyler

01-23-2014: Conference Call between U.S. EPA and FutureGen Alliance dated 1/23/2014 "Informal Request (IR) #7 (IR7_01-23-2014)"

Requests based on the text application

IR #	Subject	Page	Doc. Sec.	Par.	EPA Comment / Question / Request	FutureGen Response	Footnote / Reference Citation
01-23-2014_1	AoR Delineation				"Please provide a shapefile of the Area of Review (AoR) delineation."	The shapefile of the AoR delineation was uploaded to the Input Advisor on January 24, 2014. (Zipped file named *FutureGen2_AoR_May2013.zip*).	
01-23-2014_2	Determination of Wellhead Pressure				"FutureGen Alliance will provide a technical report regarding the wellhead pressure calculations used to come up with surface-injection pressures."	A memorandum provided in Appendix A is intended to clarify the approach used to calculate wellhead pressure from the maximum pressure allowed at the top of the injection interval in response to EPA request IR#3 10-01-2014_3. EPA reviewers had used a CO_2 density corresponding to conditions at the plant and applied it to the fluid column in the injection well to estimate the pressure difference between the wellhead and the top of the injection interval. Because the CO_2 is beyond or near its critical point, the flow is not incompressible, and density of the fluid will change all along the flow path with changes in temperature and pressure. A better estimate of the pressure difference between the wellhead and injection interval therefore requires a numerical integration, which accounts for the changing density. In addition, the fluid is also subject to frictional losses, which will offset some of the hydrostatic head in the well while the fluid is flowing. PNNL has used a computer program called CO2Flow (the software documentation is provided as an attachment) to calculate pressure changes along the pipeline and injection well. In this memorandum, an example calculation for the FutureGen 2.0 site is described. For the case presented, the pressure at the top of the injection interval, at a depth of 3,850 ft below ground surface, is considered to be equal to **90% of the fracture pressure**[1] giving a maximum pressure of **2,252 psia** at that location. Under the conditions assumed, the average specific weight of the CO_2 in the well would be 40.0 lb/ft^3, which corresponds to a hydrostatic pressure difference of **1,070 psi** from the wellhead to the top of the injection interval. Taking frictional losses into account, the CO_2Flow program calculates a total pressure difference of **890 psi** between these two points.	[1] FutureGen Alliance used a conservative Fracture Pressure equal to 0.65 psi / ft. Therefore, a value of 0.585 psi/ft (90% of 0.65 psi/ft) was used to calculate the maximum injection pressure specified in the numerical model. 2,252.3 psi was determined as the maximum injection pressure that the model would allow. This limiting value was assigned at the top of the perforated interval (depth of 3,850 ft bgs) based on the following calculation: 0.585*3,850=2,252.3 psi.

01-23-2014: Conference Call between U.S. EPA and FutureGen Alliance dated 1/23/2014, "Informal Request (IR) #7 (IR7_01-23-2014)"

Requests based on the text application

IR #	Subject	Page	Doc Sec.	Par.	EPA Comment / Question / Request	FutureGen Response	Footnote / Reference Citation
01-23-2014_3	Protection of USDW and AoR determination				FutureGen Alliance committed in RAI#11-14-2013_018 to provide results of an alternative method used to determine if the maximum extent of the predicted supercritical carbon dioxide ($scCO_2$) plume is also protective of the lowermost underground source of drinking water (USDW) from the induced reservoir pressure front at the FutureGen 2.0 site. Sensitivity cases for non-hydrostatic initial conditions should also be explored.	As discussed in a previous response to EPA's Request for Additional Information (RAI#11-14-2013_018), the FutureGen Industrial Alliance Inc. explored an alternative method of determining whether the AoR determination, which was based on the maximum extent of the predicted supercritical carbon dioxide ($scCO_2$) plume, is also protective of the lowermost underground source of drinking water (USDW) from the induced reservoir pressure front at the FutureGen 2.0 site. An extensive explanation including a description of the analytical approach, the model and the results is provided as an attachment. The scenario investigated is focused brine leakage along damaged plugged and abandoned or poorly constructed wells. A recent study published by Lawrence Berkeley National Laboratory (LBNL) researchers detailed an approach for assessing well leakage scenarios that includes an analytical model for multi-layered systems. A common limitation of simple well leakage assessments is that they neglect the impact of permeable units below the USDW. The presence of these permeable units can act as thief zones and reduce the flux of brine to the upper layers. There are three major permeable units at the site between the primary caprock and the lowermost USDW. The closest well that penetrates the caprock outside the predicted $scCO_2$ plume extent (~2 km) is located 26 km away. Brine flux into the permeable layers and USDW was estimated using the LBNL analytical model for wells at two locations (2 km and 26 km). Layer thicknesses at the site were used along with conservative estimates for their hydraulic properties. The effective permeability range for the zone around a damaged, plugged, and abandoned or poorly constructed well is not well constrained; however, researchers have categorized these wells by leakage potential (low, medium, high, and extreme). The highest permeabilities published for the High and Extremely High leakage potential categories were used for conservative estimates. Simulation results of these cases showed very small volumes of brine leakage into the lowermost USDW at the two well locations. Most of the focused leakage from the reservoir discharges into the first permeable unit above the caprock. **This analysis indicates that the AoR defined by the maximum predicted extent of the $scCO_2$ plume would also be protective of the USDWs from the induced pressure front under these scenarios**	

Appendix A

IR 01-23-2014_2

Additional Information Regarding

Determination of Wellhead Pressure

Description of Approach and Results

Summary

This memorandum is intended to clarify the approach used to calculate wellhead pressure from the pressure at the top of the injection interval in response to EPA request IR 01-10-2014_3. EPA reviewers had used a CO_2 density corresponding to conditions at the plant and applied it to the fluid column in the injection well to estimate the pressure difference between the wellhead and the top of the injection interval. Since the CO_2 is beyond or near its critical point, the flow is not incompressible, and density of the fluid will change all along the flow path with changes in temperature and pressure. A better estimate of the pressure difference between the wellhead and injection interval therefore requires a numerical integration which accounts for the changing density. In addition, the fluid is also subject to frictional losses which will offset some of the hydrostatic head in the well while the fluid is flowing. PNNL has used a computer program called CO2Flow to calculate pressure changes along the pipeline and injection well. In this memorandum, an example calculation for the FutureGen 2.0 site is described. For the case presented, the pressure at the top of the injection interval, at a depth of 3850 feet below the ground surface, is considered to be equal to 90% of the fracture pressure, giving a maximum pressure of 2252 psia at that location. Under the conditions assumed, the average specific weight of the CO_2 in the well would be 40.0 lb/ft^3, which corresponds to a hydrostatic pressure difference of 1070 psi from the wellhead to the top of the injection interval. Taking frictional losses into account, the CO2Flow program calculates a total pressure difference of 890 psi between these two points.

Several aspects of a geological carbon dioxide sequestration project require the calculation of expected conditions along the flow path from the fluid source (e.g. a power plant with CO_2 capture), through pipelines and equipment, down an injection well, and ultimately to the repository formation. The computer program CO2Flow was written to support scoping analyses, permitting, and system design associated with geological carbon dioxide sequestration. The program estimates pressure drop and fluid state evolution as CO_2 moves through pipelines and injection tubing. A steady state, one-dimensional flow model is used to calculate the pressure drop along a discrete number of pipeline or well elements. For a more detailed description, please see FG-02-RPT-0003 [1]. Basic features of the CO2Flow program have been checked using hand calculations, and predictions for full well simulations have been validated by comparison to data from injection tests at the AEP Mountaineer test site near New Haven, West Virginia.

For the FutureGen 2.0 project, the flow path includes a pipeline 28.2 miles in length, followed by a vertical well section that extends to a depth of 3184 feet below the ground surface, followed by a curved segment having a radius of 830 feet leading to the final horizontal well segment. The current design calls for the perforated well section to begin in the curved segment, which places the top of the injection interval somewhat higher than the horizontal portion of the well. A linear distance of 773 ft along the curved segment to the beginning of the perforations corresponds to a total depth of 3850 feet below the ground surface.

The pressure boundary condition for a calculation encompassing the entire flow path from fluid source to repository is generally the pressure at the top of the perforated well section required to push a given flow rate of fluid into the geological formation. The pressure required at the top of the perforated injection interval will vary over the course of injection operations as the formation is pressurized by injection and then relaxes during outages. The fluid temperature is usually specified at the CO_2 source. In such a case, the calculation marches from the fluid source to the top of the injection interval, and the pressure at the source is iterated until the required pressure at the top of the injection interval is met.

The flowing fluid is subject to frictional losses in both the pipeline and injection well tubing. Hydrostatic pressure changes are also accounted for, although the average slope of the proposed FutureGen 2.0 pipeline is small, with only a 185 ft climb from the plant to the wellhead. The majority of the pressure change as the fluid moves down the injection well is due to hydrostatic effects.

When the CO_2 travels along the pipeline from the plant, it is cooled by exchange of heat with the surroundings. The rate of cooling depends primarily upon the temperature of the surroundings and the thermal conductivity of the soil in which the pipeline is buried, but also on the fluid velocity, which is in turn a function of the pressure along the flow path between the plant and wellhead.

When injection is first initiated, significant heat transfer between the injected fluid and the rock surrounding the vertical well is expected to moderate the temperature of the fluid and pull it towards the formation temperature at depth. However, the rate of heat transfer is expected to decrease over time, as a zone of rock around the well moves closer toward thermal equilibrium with the fluid. A limiting case after long time periods of steady injection is therefore considered to be adiabatic flow of fluid in the well. Under these conditions, the fluid temperature moving down the well still changes due to Joule-Thomson effects.

Well and pipeline flow simulations were carried out for a number of conditions, covering expected injection pressures, fluid flowrates, and seasonal temperature variations. Soil thermal conductivity depends upon the soil composition and the water content, which will vary with the season. A range of soil thermal conductivities was therefore used in the simulations in order to bracket the rate of heat transfer expected in the pipeline. Extreme high and low values of 2.6 and 0.35 W/m K are suggested by Kreith and Bohn [2]. High and low values of 1.25 and 0.50 W/m K are likely more representative of the agricultural soil and moisture ranges expected along the FutureGen pipeline route. STOMP simulations encompassing planned operating schedules indicate that injection pressures will climb rapidly toward the maximum defined by the fracture pressure over a period of months. Therefore, the conditions chosen to be most representative of long, steady injections were those of nominal flow rate (1.1 MMT/year) and maximum pressure at the top of the injection interval (90% of estimated fracture pressure).

Table 1 shows input parameters for a representative case examined using the CO2Flow program. Table 2 shows calculated (or specified) CO_2 temperatures and pressures at the plant, wellhead, and top of the injection interval. The total CO_2 flow is assumed to be split evenly between four identical wells. This case assumes adiabatic conditions in the wells themselves. This calculation does not include any pressure drop due to throttling or control valves. These will likely be included in the final system in order to control the pressure and distribute flow between the four injection wells. If a given pressure drop were taken across control valves at the wellhead, then the pressure in the pipeline and at the plant would be higher by approximately that amount (not exactly by that amount, since the velocities and frictional losses in the pipeline would change slightly due to the change in fluid density).

Table 2 also includes the fluid specific weight at various points in the flow path, according to the local state variables and the Span and Wagner equation of state [3]. A rough estimate of the hydrostatic head in the well can be made by using the arithmetic average of the fluid specific weights at the wellhead and top of the injection interval, 40.0 lb/ft^3. The pressure difference thus estimated for a vertical distance of 3850 feet between the wellhead and the top of the injection interval would be 3850 ft × 40.0 lb/ft^3 = 154,000 lb/ft^2 = 1070 psi. This value is somewhat greater than the pressure difference of 890 psi between these two points calculated by the CO2Flow program, because it does not include any frictional losses.

Table 1: Input parameters for example pipeline and well case

Average annual flow rate	1.10	MMT/yr
System availability	0.85	
Maximum required injection pressure	2252	psia
Pipeline length	28.2	miles
Pipeline slope (rise/run)	0.00124	
Pipeline element length (for numerical integration)	40	m
Fluid temperature at plant	113	F
Average soil surface temperature (summer)	79.2	F
Soil thermal conductivity	0.5	W/m K
Pipeline cover depth	5	ft
Pipeline inside diameter	10.136	in
Pipeline outside diameter	10.75	in
Length of vertical well segment	3184	ft
Well curved segment radius of curvature	830	ft
Distance along curved segment to perforations	773	ft
Well element length (for numerical integration)	1	m
Injection tubing inside diameter	2.922	in
Pipe absolute roughness (pipeline and well tubing)	4.6E-5	m

Table 2: Calculated fluid conditions at various points for example case

Location	**Temperature (°F)**	**Pressure (psia)**	**Specific weight (lb/ft^3)**
Plant	113	1590	35.9
Wellhead	101	1360	38.1
Top of injection interval	130	2250	41.9

References

1. Stewart, M.L., White, M.D., and Stewart, C.W., "CO2Flow Software Documentation: Hydraulic Model for CO2 Pipelines and Injection Wells". FutureGen 2.0 Project: FG-02-RPT-0003.
2. Kreith, F.B.M., *Principles of heat transfer*. 6th / Frank Kreith, Mark S. Bohn. ed. 2001, Australia: Pacific Grove, Calif. xviii, 700 p.

3. Span, R. and W. Wagner, "A new equation of state for carbon dioxide covering the fluid region from the triple-point temperature to 1100 K at pressures up to 800 MPa". *Journal of Physical and Chemical Reference Data*, 1996. 25(6): p. 1509-1596.

Attachments

The following two stand-alone reports are attached:

- **CO2Flow Software Documentation: Hydraulic Model for CO2 Pipelines and Injection Wells**
- **Analysis of Impacts on Lowermost USDW from Focused Leakage of Brine from Plugged and Abandoned or Poorly Constructed Wells at the FutureGen 2.0 Site**

FG-02-RPT-0003

FutureGen™ ALLIANCE

Clean Energy for a Secure Future

DOE Award Number/Recipient:
DE-FE0001882, FutureGen Industrial Alliance, Inc.

CO2Flow Software Documentation: Hydraulic Model for CO_2 Pipelines and Injection Wells

January 2014

Acknowledgment: This material is based upon work supported by the Department of Energy under Award Number DE-FE0001882.

Contact Information:
FutureGen Industrial Alliance, Inc.
1001 Pennsylvania Avenue, NW
Sixth Floor
Washington, D.C. 20004
202-280-6019
Email: info@FutureGenAlliance.org
Homepage: www.FutureGenAlliance.org

FG-02-RPT-0003

CO2Flow Software Documentation: Hydraulic Model for CO2 Pipelines and Injection Wells

ML Stewart
MD White
CW Stewart

Prepared by
FutureGen Industrial Alliance, Inc.
1101 Pennsylvania Avenue, NW
Washington, D.C. 20004
DOE Award Number DE-FE0001882

January 2014

Contents

1.0 Introduction

The CO2Flow computer program was written to support scoping analyses, permitting, and system design associated with geological carbon dioxide (CO_2) sequestration. The program estimates pressure drop and fluid-state evolution as CO_2 moves through pipelines and injection tubing. A simple, steady-state, one-dimensional flow model was used to calculate the pressure drop along a discrete number of pipeline or well segments. The program is written in Fortran90.

2.0 Theory and Method

2.1 Balance Equations

With inlet conditions given (i.e., plant CO_2 delivery pressure and temperature for a pipeline or wellhead conditions for the well), the pressure at distance *j* along the pipe is given by

$$p_j = p_{j-1} - \Delta L\left[\frac{fG(V_j + V_{j-1})}{4D} - g\frac{(\rho_j + \rho_{j-1})}{2}\sin\alpha + \frac{G}{\Delta L}(V_j - V_{j-1})\right] \quad (1)$$

where
p_j = pressure at the end of length element j (Pa)
p_{j-1} = inlet pressure for length element j (Pa)
ΔL = element length = L/N for uniform elements (m)
L = total length (m)
N = number of uniform length elements
f = Darcy-Weisbach friction factor
G = mass flux = ρV, constant in the steady state (kg/s m^2)
G = $\dot{m}/A$
$\dot{m}$ = mass flow rate (kg/s)
A = cross-sectional area of pipe or injection tubing (m^2)
V = fluid velocity (m/s)
V = G/ρ
ρ = fluid density (kg/m^3)
D = pipe or injection tubing inside diameter (m)
g = acceleration due to gravity (m/s^2)
α = orientation angle of the flow (radians): 0 - horizontal, $\pi/2$ - vertical

Equation (1) is derived from a momentum balance. The three terms in brackets on the right-hand side account for frictional forces, gravity forces, and fluid acceleration, respectively.
The friction factor is calculated using the Shacham equation, which is explicit in *f* and accurate to ±1% (Robinson 1996). The equation is given by

$$f = \left\{-2\log\left[\frac{\varepsilon/D}{3.7}\right] - \frac{5.02}{\text{Re}}\log\left(\frac{\varepsilon/D}{3.7} + \frac{14.5}{\text{Re}}\right)\right\}^{-2} \quad (2)$$

where ε = pipe roughness (m)
Re = Reynolds number

$$\mathrm{Re} = \frac{\rho V D}{\mu}$$

μ = fluid viscosity (N-s/m^2)

The internal energy at the end of length element j is calculated by the following equation, derived from an energy balance

$$u_j = u_{j-1} + \left[\frac{Q_j}{\dot{m}} \Delta L - \left(\frac{p_j}{\rho_j} - \frac{p_{j-1}}{\rho_{j-1}} \right) - \frac{1}{2}(V_j^2 - V_{j-1}^2) + g \Delta L \sin \alpha \right] \tag{3}$$

where u_j = internal energy at the end of length element j (J/kg).
u_{j-1} = internal energy at the inlet of length element j (J/kg)
Q = rate of heat transfer per unit length into the CO_2 (w/m)

The first term in brackets on the right-hand side of Equation (3) accounts for the heat transfer into the CO_2 stream, the second term is the change in potential energy due to pressure, the third term is the change in kinetic energy of the flow, and the last term is the change in gravitational potential energy. Viscous work is ignored, as is customary for flow in pipes (White 1994, p. 150).

2.2 Fluid-State Information

CO_2 density and internal energy are estimated from temperature and pressure using the CO_2 state equation according to (Span and Wagner 1996). The state equation also allows the calculation of phase distribution for conditions of vapor/liquid equilibrium. For the purposes of current well and pipeline calculations the CO_2 is assumed to be either a liquid or supercritical fluid, and the calculation is terminated if two-phase conditions occur.

Viscosity is estimated from the average temperature and density in each pipe element using the correlation of Fenghour et al. (1998).

Two-phase flow could be simulated in future versions of the model; however, it is a challenging technical problem. Momentum sinks during two-phase flow depend upon factors such as phase distribution, flow orientation with respect to gravity, and flow regime (e.g., frothy, annular flow, and slug flow). Different correlations, with widely varying uncertainties and levels of complexity, are typically used to describe these various conditions.

2.3 Effects of Heat Transfer

Heat transfer to the surroundings is calculated by

$$Q = U\left(T_i - T_\infty\right) \tag{4}$$

where U = overall heat conductance per unit length from fluid to ultimate heat sink (w/m-K)
T_∞ = temperature of the ultimate heat sink (C)

For horizontal pipelines, the ultimate heat sink is the soil surface. Monthly mean temperatures at 4 in. below the surface typically define the bounding heat sink temperatures. Steady-state heat transfer is assumed with the thermal resistance of the steel pipe wall assumed to be negligible (i.e., the pipe is assumed to have the same temperature as the fluid). Under these assumptions the conductance, as defined by (Kreith and Bohn 2001), is

$$U = \frac{2\pi \Delta L}{\frac{\cosh^{-1}(2z / D_o)}{k_s} + \frac{\ln(1 + t / D_o)}{k_i}} \tag{5}$$

where

k_s	=	soil thermal conductivity (w/m-K)
z	=	depth of pipe centerline below soil surface (m)
D_o	=	outside diameter of steel line pipe (m)
t	=	thickness of insulation (m)
k_i	=	thermal conductivity of insulation (w/m-K)

The thermal conductivity of soil can vary widely. Typically, values of 2.6 and 0.35 W/m K have been used for wet and dry soil, respectively (Kreith and Bohn 2001). To bound the heat-transfer estimates, the higher conductivity was used for winter cases, during which the temperature difference between the pipeline and its surroundings would be the greatest. The lower conductivity was used for summer cases.

NOTE: While the CO_2 flow and pressure model supports simulation of heat transfer from the wellbore into surrounding rock as described below, this feature has not been validated in the current model version and should be used for information purposes only.

Heat transfer from the well will be a transient phenomenon, as a temperature front moves radially outward, ultimately to rock at great distances from the well bore. Equivalent heat conductance from the well outward is defined at a given elapsed time after injection starts by

$$U(t) = \frac{Q_{FD}(t)}{T_i - T_\infty} \tag{6}$$

where

$U(t)$	=	equivalent heat conductance at time t after flow begins (w/m-K)
$Q_{FD}(t)$	=	heat-transfer rate per unit length at time t (w/m)

It the past, equivalent conductance from the well into the rock was roughly estimated using a greatly simplified one-dimensional radial transient finite difference model in a separate spreadsheet model (which has not been formally reviewed and is not documented in detail here). Although not part of the CO2Flow program, the methodology previously used to estimate the conduction from the well is briefly discussed here for context. Besides assuming uniform rock properties all along the depth of the well, the simple transient model also assumed a constant temperature boundary condition at the outside surface of the well casing, while in reality the driving temperature would change as a function of time and depth. The finite difference model ignored the relatively small thermal resistance of the injection tube wall, casing wall, and the fluid in the annulus between them by assuming that the temperature at the outside surface of the casing was equal that of the carbon dioxide. The thermal conductivity of the concrete seal was assumed equal to that of the surrounding rock. Because the timescale of transient temperature evolution in the rock adjacent to the well is much longer than the fluid residence time in the injection tube, a pseudo-steady heat-transfer assumption was used to estimate the effects of heat transfer on the fluid temperature at a given point in time.

While not expected to give a precise estimate of the actual transient-heat transfer from the injection well bore to the surrounding rock, the method described above may be useful to provide a rough approximation. The rate of heat transfer is expected to diminish over time as the temperature of the rock near the well approaches thermal equilibrium with the fluid at a given depth. Therefore, adiabatic conditions in the well have been considered a bounding case to approximate conditions after long periods of injection.

2.4 Numerical Method

The temperature and pressure at the end of each pipe element are estimated iteratively using the Newton-Raphson method. When convergence is achieved in both state variables, the program marches to the next pipe element. This process is repeated until the entire length has been traversed. In calculations with an injection well following a pipeline, the conditions exiting the pipeline are used at the wellhead inlet. No effects of fittings, valves, elbows, or manifolds are included in the current calculation.

3.0 Running the Program

3.1 Setup and Compilation

Source code for the CO2Flow program is contained in a single source file, CO2Flow.f90. The code has most recently been used with the Intel Fortran compiler version 11.1.069 on a cluster running Red Hat Linux Client release 5.9. Using that compiler, the program can be compiled with the following command:

```
ifort –o CO2Flow.x CO2Flow.f90
```

The program also makes use of the physical properties file co2_prop.dat. This file is used to store a table of physical properties at a finite number of state points that the program interpolates between. All applications of the CO2Flow program up to this point have used the same physical properties file.

The physical properties file is generated by a separate utility program in co2_eos.f90, which can be compiled in a manner similar to CO2Flow:

```
ifort –o co2_eos.x co2_eos.f90
```

When co2_eos.x is executed, it reads in a set of state points specified in co2_pt.dat. It is only necessary to compile and run the co2_eos.x program once. As long as the co2_prop.dat file remains accessible to the CO2Flow.x program, any number of flow simulations can be run using the same file. The number and range of state points specified could be changed to improve the fidelity of physical properties values used during CO_2 flow simulations.

The files CO2Flow.f90, co2_eos.f90, and co2_pt.dat are configuration-managed using the revision control system known as Mercurial. Mercurial generates a unique hash for each code changeset. As of this revision of the program documentation, the current program changeset is 1:02148dfedd94.

3.2 Execution

The executable program CO2Flow.x accepts one command line argument, which is the name of the input file. A typical execution command on a Linux cluster running the Bash shell would be:

```
./CO2Flow.x input.inp
```

where "input.inp" is the input file.

Multiple runs using different input files may be un using a simple script such as:

```
files=$(ls *.inp)
for filename in $files; do
echo processing $filename
./CO2Flow.x $filename
done
```

This script will execute the CO2Flow program using all of the files in the present directory having .inp extensions as input files.

3.3 Input

Program input parameters are currently read from an ASCII text file using Fortran 90-compliant list-directed sequential READ statements. With this input method, input parameters need not be included in any specific order, and parameters can often be added while maintaining compatibility with old input decks. An example input file is included below.

```
&INPUTPARAMS

!  General Parameters

MassFlow     = 41.04   ![kg/s] Mass flow rate in pipeline

StartPress   = 12.41   ![MPa] Pressure at beginning of first pipe segment
StartTemp    = 4.4     ![C] Temperature at beginning of first pipe segment

IteratePress = .true.  !Flag to iterate pressure to meet injection requirements
ReqPress     =         18.22   ![MPa] Minumum Required well bottom pressure
PressTol     =         0.01    ![MPa] Pressure target tolerance - allowable pressure above target

!  First Pipe Segment:  Vertical well segment

FracFlow(1)     =      0.5      !Fraction of total flow handled by this pipe segment
Length(1)       =      975.359968788481       ![m] Length of pipe segment
DiscLength(1)   =      1        ![m] Discretization of pipe segment (dx)
Diameter(1)     =      0.07422 ![m] Internal pipe diameter
OuterDiam(1)    =      0        ![m] Outer pipe diameter
IsVertical(1)   =      .true.  !(.true. or .false.) Flag for vertical pipe
Slope(1)        =      0        ![]  Slope of segment, rise over run, negative for downslope
PipeRough(1)    =      0.000046        ![m] Absolute roughness of pipe wall (comercial steel)

SurrTemp0(1)    =      12.257936869826        ![C] Surrounding temperature zero order term
```

```
SurrTemp1(1)       =      0.0182  ![C] Surrounding temp first order term wrt distance (linear
variation)
HeatXFer(1)        =      'none'  !Type of heat transfer calculation
HeatXFerCoeff(1) =        0       ![W/m K] Thermal conductivity of material around pipe

InsThick(1)        =      0       ![m] Thickness of insulation around pipe
InsCond(1)         =      0       ![W/m K] Thermal conductivity of pipe insulation


!  Second Pipe Segment:  Curved well segment

FracFlow(2)        =      0.5     !Fraction of total flow handled by this pipe segment
Length(2)          =      397.386325221518       ![m] Length of pipe segment
DiscLength(2)      =      1       ![m] Discretization of pipe segment (dx)
Diameter(2)        =      0.07422 ![m] Internal pipe diameter
OuterDiam(2)       =      0       ![m] Outer pipe diameter
VCurve(2)    =   .true.   !(.true. or .false.) Flag for curved pipe segment
Slope(2)           =      0       ![]  Slope of segment, rise over run, negative for downslope
PipeRough(2)       =      0.000046       ![m] Absolute roughness of pipe wall (comercial steel)

SurrTemp0(2)       =      12.257936869826        ![C] Surrounding temperature zero order term
SurrTemp1(2)       =      0.0182  ![C] Surrounding temp first order term wrt distance (linear
variation)
HeatXFer(2)        =      'none'  !Type of heat transfer calculation
HeatXFerCoeff(2) =        0       ![W/m2 K] Effective heat transfer coefficient to surroundings

InsThick(2)        =      0       ![m] Thickness of insulation around pipe
InsCond(2)         =      0       ![W/m K] Thermal conductivity of pipe insulation
/

CaseID MorgWell_080712_1
```

Comments in the above input file give units and a brief description of each of the normally used input parameters. The use of some input parameters is explained in more detail below.

IteratePress, StartPress, ReqPress, and PressTol

The program moves sequentially from one end of the flow stream to the other. State variables at the end of the last pipe segment are therefore determined by the state variables at the beginning of the first segment and the various other model parameters. When the parameter IteratePress is set to ".false.", this calculation is performed once. In some cases it is desirable to specify the pressure at the end of the last segment (e.g., the required pressure at the bottom of an injection well) and automatically adjust the inlet pressure in order to achieve this value. This is done by setting IteratePress to ".true.". In this case, StartPress is simply used as in initial value for the pressure at the inlet of the first pipe segment. The desired pressure at the end of the last segment is input as parameter ReqPress. The parameter PressTol specifies how close the pressure must be to the required value. Note: the pressure at the end of the last segment will always be above the required pressure in a converged solution.

IsVertical()

The IsVertical flag is used to specify a vertical pipe segment with a value of ".true.". in this case the Slope() parameter is ignored and normally set to zero. Any finite value of slope (rise over run) may be specified when IsVertical is set to ".false.". A negative value for Slope signifies a downward sloping pipe run.

SurrTemp0() and SurTemp1()

The SurrTemp parameters allow a linear temperature relationship to be specified as a function of the linear distance along the current pipe segment. The temperature of the ultimate heat sink surrounding the pipe therefore has the form

$$T = SurrTemp0 + SurTemp1 \cdot x \tag{7}$$

For a single, constant temperature along the entire length of the pipe segment, SurTemp1() would be set to zero.

HeatXFer()

The parameter HeatXFer() is used to specify the heat-transfer model to be used for a given pipe segment. There are two valid character string values for this parameter that result in heat transfer over the pipe segment. Setting the parameter to 'surface' specifies the use of the Kreith and Bohn approximation for heat transfer from a buried pipeline (Kreith and Bohn 2001). Setting the parameter to 'coefficient' specifies the use of a single effective heat-transfer coefficient, which is input as the parameter HeatXFerCoeff(). Any other value for the parameter HeatXfer() will result in adiabatic conditions over the pipe segment (i.e., zero heat flux to surroundings).

InsThick() and InsCond()

For non-adiabatic models, the resistance to heat transfer may be increased by adding a layer of insulation around the pipe using parameters InsThick() and InsCond(), which specify the thickness and thermal conductivity of the insulation, respectively.

VCurve() and CurveRad()

VCurve() is a logical flag that specifies a curved piping segment when its value is ".true.". The default value is ".false.". VCurve() = ".true." is used to specify a section of pipe which curves from vertical to horizontal in a vertical plane. This feature represents a well in which directional drilling has been used to transition between a vertical access well and a horizontal injection zone. Friction, gravity, and heat-transfer effects are calculated for each element of the curved section. By default, it is assumed that a full 90 degree bend (one quarter of a perfect circle) is accomplished over the length of the pipe segment. In this case the radius of curvature would equal the length of the pipe segment divided by $\pi/2$. It is also possible to specify a different radius of curvature through the parameter CurveRad(), which specifies the radius in meters.

The example input file includes two pipe segments: one vertical and one curved. The program version supports up to five sequential segments, but this value could be easily increased in the Fortran code if necessary. The program begins at the first segment, and proceeds until it encounters a segment with zero length (zero is the default value for the Length() parameter).

3.4 Output

Simulation results are output as ASCII text files. The output files have a tabular format, with a column for each output variable and a row for each discrete element along each pipe segment. Excerpts from an example output file (corresponding to the input file given in the previous section) are shown in Appendix A.

"Distance" is the linear distance in meters along the current pipe segment. "Pressure", "Temperature", "Density", and "Viscosity" are the local fluid properties in the units shown. "Int Energy" is the local fluid specific internal energy in J/kg, while "Entropy" is the local fluid specific entropy in J/(kg K).

"Int Heat", "Int Fric DP", and "Int Grav DP" are, respectively, total heat transferred, total pressure drop due to friction, and total pressure change due to gravity, integrated over the length of the pipe segment. These values are typically used to check relative magnitudes of the various effects and verify consistency and reasonableness of the results.

3.5 Limitations

The current version of the code limits the number of consecutive piping segments to five. Input and output filenames are limited to 30 characters.

As described in Section 2.2, the current version of the code is limited to flow regimes in which the liquid-vapor transition line is not crossed at any point along the flow path.

4.0 References

Fenghour A, WA Wakeham, and V Vesovic. 1998. "The viscosity of carbon dioxide." *J. Phys. Chem. Ref. Data*, 27(1):31-41.

Kreith F and MS Bohn. 2001. *Principles of Heat Transfer.* 6th ed. PWS Publishing Co.

Robinson RN. 1996. *Chemical Engineering Reference Manual.* Professional Publications, Inc.

Span R and W Wagner. 1996. "A New Equation of State for Carbon Dioxide Covering the Fluid Region from the Triple-Point Temperature to 1100K at Pressures up to 800 MPa." *J. Phys. Chem. Ref. Data*, Vol. 25, 1509-1596.

White FM. 1994. *Fluid Mechanics*. 3rd ed. New York: McGraw-Hill. xiii, 736 p.

Appendix A

Output File Format

Appendix A

Output File Format

```
Distance    Pressure    Temperature Density     Int Energy  Entropy     Viscosity   Velocity    Int Heat    Int Fric DP Int Grav DP
 m          MPa         C           kg/m^3       J/kg        J/kg K     N s/m2       m/s        J/kg         MPa         MPa
 0.0000E+00  1.0478E+01  4.4000E+00  9.5436E+02 -3.1274E+05 -1.7477E+03  1.0718E-04  4.9698E+00
 1.0000E+00  1.0484E+01  4.4058E+00  9.5437E+02 -3.1273E+05 -1.7477E+03  1.0718E-04  4.9697E+00  0.0000E+00 -2.8060E-03  9.3622E-03
 2.0000E+00  1.0491E+01  4.4116E+00  9.5438E+02 -3.1273E+05 -1.7477E+03  1.0718E-04  4.9697E+00  0.0000E+00 -5.6121E-03  1.8725E-02
 3.0000E+00  1.0498E+01  4.4174E+00  9.5439E+02 -3.1273E+05 -1.7477E+03  1.0719E-04  4.9696E+00  0.0000E+00 -8.4180E-03  2.8087E-02
 4.0000E+00  1.0504E+01  4.4233E+00  9.5439E+02 -3.1272E+05 -1.7477E+03  1.0719E-04  4.9696E+00  0.0000E+00 -1.1224E-02  3.7450E-02
 5.0000E+00  1.0511E+01  4.4291E+00  9.5440E+02 -3.1272E+05 -1.7477E+03  1.0719E-04  4.9695E+00  0.0000E+00 -1.4030E-02  4.6812E-02
.
.
.
 9.7200E+02  1.6912E+01  1.0127E+01  9.6408E+02 -3.0976E+05 -1.7377E+03  1.0993E-04  4.9196E+00  0.0000E+00 -2.7137E+00  9.1471E+00
 9.7300E+02  1.6918E+01  1.0133E+01  9.6409E+02 -3.0976E+05 -1.7376E+03  1.0993E-04  4.9196E+00  0.0000E+00 -2.7165E+00  9.1566E+00
 9.7400E+02  1.6925E+01  1.0139E+01  9.6410E+02 -3.0976E+05 -1.7376E+03  1.0994E-04  4.9195E+00  0.0000E+00 -2.7193E+00  9.1660E+00
 9.7500E+02  1.6932E+01  1.0145E+01  9.6411E+02 -3.0975E+05 -1.7376E+03  1.0994E-04  4.9195E+00  0.0000E+00 -2.7221E+00  9.1755E+00
 9.7600E+02  1.6938E+01  1.0151E+01  9.6412E+02 -3.0975E+05 -1.7376E+03  1.0994E-04  4.9194E+00  0.0000E+00 -2.7249E+00  9.1849E+00
Distance    Pressure    Temperature Density     Int Energy  Entropy     Viscosity   Velocity    Int Heat    Int Fric DP Int Grav DP
m           MPa         C           kg/m^3      J/kg        J/kg K      N s/m2      m/s         J/kg        MPa         MPa
 0.0000E+00  1.6938E+01  1.0151E+01  9.6412E+02 -3.0975E+05 -1.7376E+03  1.0994E-04  4.9194E+00
 1.0000E+00  1.6945E+01  1.0157E+01  9.6413E+02 -3.0975E+05 -1.7376E+03  1.0994E-04  4.9194E+00  0.0000E+00 -2.7276E+00  9.1944E+00
 2.0000E+00  1.6952E+01  1.0163E+01  9.6414E+02 -3.0974E+05 -1.7376E+03  1.0995E-04  4.9193E+00  0.0000E+00 -2.7304E+00  9.2039E+00
 3.0000E+00  1.6958E+01  1.0169E+01  9.6415E+02 -3.0974E+05 -1.7376E+03  1.0995E-04  4.9193E+00  0.0000E+00 -2.7332E+00  9.2133E+00
 4.0000E+00  1.6965E+01  1.0175E+01  9.6416E+02 -3.0974E+05 -1.7376E+03  1.0995E-04  4.9192E+00  0.0000E+00 -2.7360E+00  9.2228E+00
 5.0000E+00  1.6972E+01  1.0181E+01  9.6417E+02 -3.0973E+05 -1.7376E+03  1.0996E-04  4.9191E+00  0.0000E+00 -2.7388E+00  9.2322E+00
.
.
.
 3.9400E+02  1.8240E+01  1.1551E+01  9.6474E+02 -3.0861E+05 -1.7336E+03  1.1006E-04  4.9163E+00  0.0000E+00 -3.8183E+00  1.1580E+01
 3.9500E+02  1.8237E+01  1.1550E+01  9.6473E+02 -3.0860E+05 -1.7336E+03  1.1006E-04  4.9163E+00  0.0000E+00 -3.8210E+00  1.1580E+01
 3.9600E+02  1.8235E+01  1.1550E+01  9.6471E+02 -3.0860E+05 -1.7336E+03  1.1005E-04  4.9164E+00  0.0000E+00 -3.8238E+00  1.1580E+01
 3.9700E+02  1.8232E+01  1.1550E+01  9.6470E+02 -3.0860E+05 -1.7336E+03  1.1005E-04  4.9165E+00  0.0000E+00 -3.8266E+00  1.1580E+01
 3.9800E+02  1.8229E+01  1.1549E+01  9.6469E+02 -3.0860E+05 -1.7336E+03  1.1005E-04  4.9165E+00  0.0000E+00 -3.8294E+00  1.1580E+01
```

Battelle
The Business of Innovation

Study or Report No. PNWD-4414

Analysis of Impacts on Lowermost USDW from Focused Leakage of Brine from Plugged and Abandoned or Poorly Constructed Wells at the FutureGen 2.0 Site

Battelle, Pacific Northwest Division
P.O. Box 999
Richland, Washington 99352

The FutureGen Industrial Alliance, Inc.
1101 Pennsylvania Avenue, NW
Washington, DC 20004
DOE Award Number DE-FE0001882

January 2014

LEGAL NOTICE

Analysis of Impacts on Lowermost USDW from Focused Leakage of Brine from Plugged and Abandoned or Poorly Constructed Wells at the FutureGen 2.0 Site

MD Williams
VR Vermeul
D Appriou
A Bonneville
JA Horner
FA Spane
TJ Gilmore

January 2014

Prepared by
Battelle, Pacific Northwest Division
P.O. Box 999
Richland, Washington 99352

Prepared for
The FutureGen Industrial Alliance, Inc.
1101 Pennsylvania Avenue, NW
Washington, DC 20004
DOE Award Number DE-FE0001882

Summary

This report documents an analysis conducted in response to a Request for Additional Information from the U.S. Environmental Protection Agency about the FutureGen Industrial Alliance, Inc.'s (Alliance's) Revision 1, *Underground Injection Control (UIC) Class VI Injection Well Permit Applications for FutureGen 2.0 Morgan County UIC Wells 1, 2, 3, and 4 SUPPORTING DOCUMENTATION*. The objective of the analysis was to assess whether an Area of Review (AoR) determination, which was based on the maximum extent of the predicted supercritical carbon dioxide ($scCO_2$) plume, is also protective of the lowermost underground source of drinking water (USDW) from the induced reservoir pressure front at the FutureGen 2.0 site. The scenario investigated is focused brine leakage along damaged plugged and abandoned or poorly constructed wells. A recent study published by Lawrence Berkeley National Laboratory (LBNL) researchers detailed an approach for assessing well leakage scenarios that includes an analytical model for multi-layered systems. A common limitation of simple well leakage assessments is that they neglect the impact of permeable units below the USDW. The presence of these permeable units can act as thief zones and reduce the flux of brine to the upper layers.

There are three major permeable units at the site between the primary caprock and the lowermost USDW. The closest well that penetrates the caprock outside the predicted $scCO_2$ plume extent (~2 km) is located 26 km away. Brine flux into the permeable layers and USDW was estimated using the LBNL analytical model for wells at two locations (2 km and 26 km). Layer thicknesses at the site were used along with conservative estimates for their hydraulic properties. The effective permeability range for the zone around a damaged, plugged, and abandoned or poorly constructed well is not well constrained; however, researchers have categorized these wells by leakage potential (low, medium, high, and extreme). The highest permeabilities published for the High and Extremely High leakage potential categories were used for conservative estimates.

Simulation results of these cases showed very small volumes of brine leakage into the lowermost USDW at the two well locations. Most of the focused leakage from the reservoir discharges into the first permeable unit above the caprock. This analysis indicates that the AoR defined by the maximum predicted extent of the $scCO_2$ plume would also be protective of the USDWs from the induced pressure front under these scenarios.

Acknowledgments

The authors would like to thank Dr. Abdullah Cihan (LBNL) for sharing his analytical model, along with test cases, for the simulations used in this report and his help on some of the cases used in this study. We also appreciated the guidance provided by Dr. Jens Birkholtzer (LBNL) on detailing the steps required for assessing this scenario. Christian Johnson (PNNL) provided a very thorough internal peer review of both the text and the simulation input/output files. Susan Ennor and Mike Parker were helpful in the editing and text processing of this report.

Acronyms and Abbreviations

Alliance	FutureGen Industrial Alliance, Inc.
AoR	Area of Review
CO_2	carbon dioxide
FGA#1	FutureGen 2.0 stratigraphic borehole
EPA	U.S. Environmental Protection Agency
km	kilometer(s)
L	liter(s)
L/m	liter(s) per meter
LBNL	Lawrence Berkeley National Laboratory
m	meter(s)
m^3	cubic meter(s)
m/s	meter(s) per second
m^3/s	cubic meter(s) per second
mD	millidarcy(ies)
MMT/yr	million metric tons per year
$scCO_2$	supercritical carbon dioxide
PNNL	Pacific Northwest National Laboratory
RAI	Request for Additional Information
UIC	Underground Injection Control
USDW	underground source of drinking water

Contents

Figures

Tables

1.0 Introduction

The FutureGen Industrial Alliance, Inc. (Alliance) prepared supporting documentation for its Underground Injection Control (UIC) Class VI permit applications for the construction and operation of four injection wells in Morgan County, Illinois, for the injection of carbon dioxide (CO_2). Upon reviewing the supporting documentation, the U.S. Environmental Protection Agency (EPA) issued several Requests for Additional Information (RAIs). RAI 11-14-2013, Regarding FG-RPT-017, Revision 1, *SUPPORTING DOCUMENTATION: Underground Injection Control Class VI Injection Well Permit Applications For FutureGen 2.0 Morgan County UIC Wells 1, 2, 3, and 4* included a comment (RAI 11-14-2013_018) about the calculation of critical pressure. It recommended that the Alliance explore alternative methods for determining critical pressure—methods such as those described by Nicot et al. (2008); Birkholzer et al. (2011); or Bandilla et al. (2012).

1.1 Objective

The objective of the analyses described in this report was to assess whether the Area of Review (AoR) determination, which was based on the maximum extent of the supercritical carbon dioxide ($scCO_2$) plume, is also protective of the lowermost underground source of drinking water (USDW) from the induced pressure front from $scCO_2$ injection.

1.2 Related Considerations

This calculation must consider the potential for brine migration into aquifers and USDWs along plugged and abandoned or poorly constructed wells that penetrate the caprock, driven by the reservoir pressure increases associated with $scCO_2$ injection. As noted by many authors, and shown in results from our injection modeling, the extent of the pressure increase during $scCO_2$ injection is larger than the extent of the $scCO_2$ plume. However, this extended region of increased pressure does not necessarily result in an increased risk to USDWs when mitigating factors are considered.

As discussed by Birkholzer et al. (2011), determination of a static critical threshold pressure for flow of brine up an open conduit or damaged borehole (e.g., substandard well completion, deteriorating seal in abandoned well, or near-borehole drilling-related formation damage) may not be applicable for cases where permeable units exist between a deep injection reservoir and lowermost USDW, because the open conduit approach does not account for lateral flow outside the conduit or casing and into these permeable zones. The effective permeability around a damaged plugged and abandoned or poorly constructed well would be smaller than in an unplugged well casing (i.e., open conduit) and would permit brine to flow into intervening permeable formations (i.e., thief zones). Birkholzer et al. (2011) stated that a model is required to analyze these dynamic and transient impacts.

At the FutureGen 2.0 site in Morgan County, Illinois, many potential thief zones exist between the injection reservoir and the lowermost USDW, including 1) the Ironton Sandstone, 2) the Potosi Dolomite (which was identified as a very challenging lost-circulation zone during drilling activities related to the FutureGen 2.0 stratigraphic borehole [FGA#1], indicating extremely high-permeability conditions), and 3) the New Richmond Sandstone.

2.0 Analytical Approach

The analysis reported here followed the approach detailed by Birkholzer et al. (2013) for analyzing the impacts of the focused leakage of brine up a damaged, plugged, and abandoned or poorly constructed well based on the pressure buildup caused by $scCO_2$ injection. The analysis used by Birkholzer et al. (2013) applied an analytical model, ASLMA (Cihan et al. 2011, 2013), which was developed specifically for these types of focused leakage problems. The ASLMA analytical model was selected for this analysis because of its capabilities and published prior use, which included verification cases with other models for these types of problems. In this study for the FutureGen2.0 site, an assessment was conducted of the impacts on the lowermost USDW from focused leakage at the closest well outside the maximum extent of the $scCO_2$ plume that penetrates the caprock; this well is the Criswell borehole at the Waverly field, which is 26 km from the center of the FutureGen 2.0 injection wells. Cases were also run for astratigraphic borehole, FGA#1 (which will be completed as a monitoring well), that is located near the maximum extent of the predicted $scCO_2$ plume approximately 2 km from the centroid of the injection well laterals. Figure 1 shows the location of the closest wells that penetrate the primary caprock above the injection reservoir around the FutureGen 2.0 site. The results of the cases run at these two selected locations can provide guidance on the adequacy of the FutureGen 2.0 site AoR, which was defined based on the maximum predicted $scCO_2$ extent in the Underground Injection Control (UIC) Permit Application, to be protective of the lowermost USDW in the context of focused brine leakage from damaged, plugged, and abandoned or poorly constructed wells.

Mount Simon Sandstone Structure Contour Surrounding FutureGen 2.0 Site

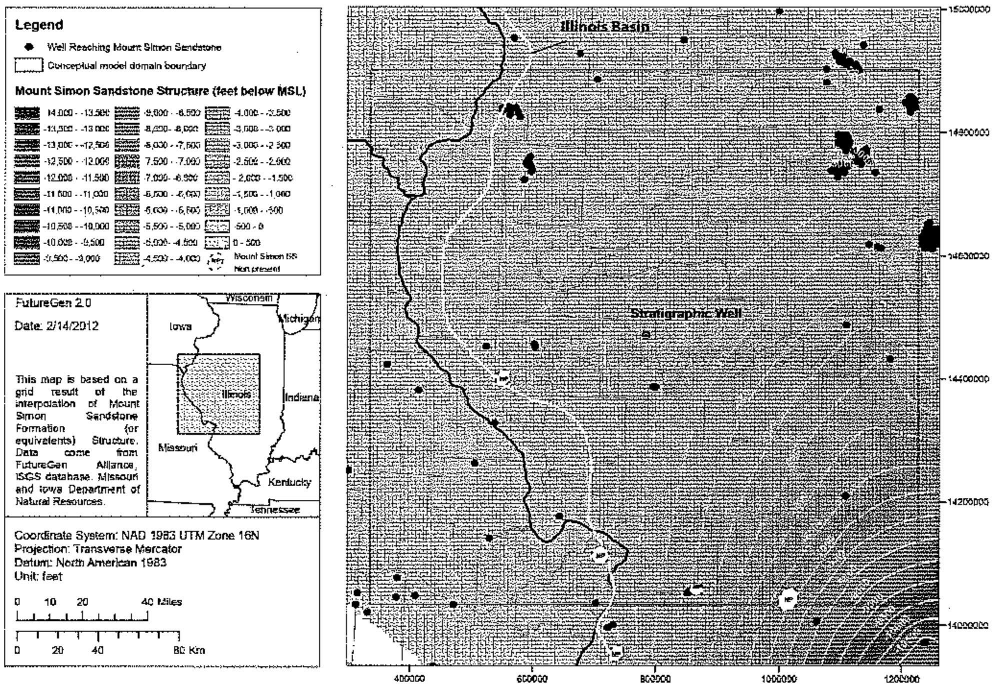

Wells Reaching the Mt Simon Ss. Closest to the FutureGen 2.0 Site

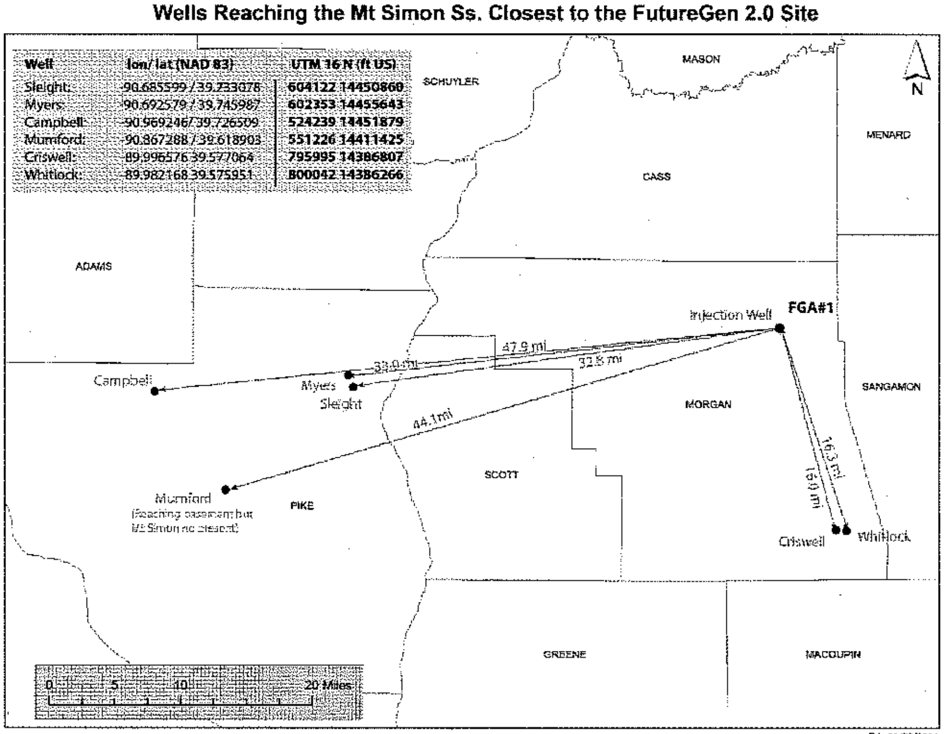

Figure 1. Location of the FutureGen 2.0 site and closest wells that penetrate the Mount Simon Sandstone.

3.0 Model Description

The ASLMA_V3 analytic model (Cihan et al. 2011), which is implemented as a Fortran 90 calculational code, was used for the analyses discussed in the report. Additional examples, of the application of ASLMA_V3 are described by Cihan et al. (2013). Pacific Northwest National Laboratory (PNNL) has obtained the ASLMA_V3 source code, executable computer file, and sample problems from the authors at Lawrence Berkeley National Laboratory (LBNL). The model applies to single-phase, isothermal fluid flow for focused leakage around wells and/or diffuse leakage through aquitards in a multilayered aquifer system that results from the transient pressure field created during reservoir injection. The model requires specification of the permeability, specific storage, and unit thickness of the reservoir, aquifers, and aquitards. Because the simulation option of solving only for focused leakage into aquifers around a borehole was used in this analysis, aquitard permeability and specific storage were not used in the model. The model also requires borehole radii and effective permeabilities for the damaged zone around the borehole for each segment of the aquifers and aquitards it encounters. Initial conditions for the model assume a hydrostatic pressure gradient. The model does not account for brine density differences, but this simplifying assumption is conservative because the volume of freshwater leakage calculated for each permeable unit would be larger than if higher-density reservoir fluid were used in the calculation.

The "ASLMA_V3.exe" executable supplied by LBNL was verified by rerunning the test cases published by Cihan et al. (2011). The test cases developed and discussed by Cihan et al. (2011) for verification included cases for comparison with earlier published models and results. The output files of the simulation runs at PNNL for these test cases were the same as the output files of these test cases supplied by LBNL.

Runs were also conducted on another version of this code, ASLMA_V3_initialheads, which allows initial hydraulic head values to be specified for each of the aquifer units. This removes the hydrostatic head initial condition limitation of the ASLMA_V3 code. The source code and executable were supplied to PNNL by the code author at LBNL. No published results of simulations with the "initialheads" version of the code or version-specific test problems were available; however, one set of input and output files was supplied by the author. We reran this case at PNNL with the supplied executable and the output files that were obtained matched the LBNL output files. Another test of this code was conducted by comparing the results of a case where the initial hydraulic head values were set to the same values as the hydrostatic head. The results of this case were similar to the results using ASLMA_V3. One initial issue in using ASLMA_V3_initialheads was the observation of oscillations in the results for very small leakage rate values (i.e., in the upper layer of the model). This oscillation issue was not encountered with the ASLMA_V3 code. We contacted the code author about this problem and he tested the problem and recommended changing a solution control parameter in the input file in a manner to reduce the round-off errors for the code. The solution in the ASLMA_V3_initialheads version involves additional terms because of the non-hydrostatic initial conditions, hence the round-off errors were causing fluctuations in the very small (practically zero) fluxes.

4.0 Model Parameters

Site data for the upper layers (Ironton to St. Peter) are limited at the FutureGen 2.0 site because the focus of the detailed characterization of the first stratigraphic borehole (FGA#1) was on the reservoir and caprock. Detailed characterization of the upper layers is planned for the next drilling campaign. Some sidewall core permeability measurements of these upper layers were used, along with published regional values or conservative estimates (i.e., using lower ranges of permeability estimates for the aquifers below the USDW).

Direct measurements of the effective permeability of plugged and abandoned or poorly constructed wells are limited. Vertical Interference Tests have recently been used to help quantify this measurement for a range of wells (e.g., Crow et al. 2010; Gasda et al. 2013; Duguid et al. 2013). Effective permeability estimates for the damaged zone around a borehole for this study were based on published ranges of groupings of wells with different leakage potentials (low, medium, high, extreme), as reported in Table 2 of Celia et al. (2011), which used the categories defined by Watson and Bachu (2008). Celia et al. (2011) used a stochastic modeling study with a large number of realizations for wells in the Wabamun Lake area of Alberta, Canada. Data from Crow et al. (2010) were also used by Celia et al. (2011) to develop these effective permeability estimates, which also highlighted the few measurements available. The high end of the High Leakage Potential Category (0.5 to 8 mD) and Extreme Leakage Potential Category (8 to 10,000 mD) (Celia et al. 2011) were investigated in this modeling effort. Single values of effective permeability for the borehole were assigned for all the aquifer/aquitard segments (instead of variable borehole permeability for each segment), which provide conservative results based on the analysis of Celia et al. (2011).

The results from this analysis are reported as the volume of fluids leaked over time from the reservoir into each of the overlying aquifers (including the St. Peter, the lowermost USDW) for the two well distances (~2 km and 26 km) using conservative estimates for the site parameters and the borehole effective permeabilities, as discussed above. Well locations are shown in Figure 1. The two wells used in this analysis were 1) the Criswell borehole at the Waverly field 26 km southeast of the center of the FutureGen 2.0 injection wells (which isthe closest borehole that penetrates the Mount Simon Formation outside the predicted $scCO_2$ plume), and 2) the FGA#1 borehole that will be completed as a monitoring well located at a distance of 2 km from the center of the injection wells, which is near the maximum extent of the predicted $scCO_2$ plume. Criswell and FGA#1 borehole diagrams are shown in Figure 2 and Figure 3, respectively.

Thicknesses and properties for the layers in the model are shown in Table 1. Layer thicknesses are taken from the characterization/stratigraphic borehole (FGA#1) drilled at the FutureGen 2.0 site (Table 6.1 of Battelle [2012]). Adjacent aquitards are lumped into a single unit as required for the model because the code input structure only allows for a sequence of alternating aquifers and aquitards. The thickness of the reservoir was calculated by combining the upper permeable portion of the Mount Simon that was targeted in the UIC permit injection model and the Elmhurst member of the Eau Claire Formation.

Hydraulic properties are not listed in Table 1 for the aquitards because flow into these units is not calculated for the focused leakage-only model of ASLMA. Aquifer property determinations for the units other than the injection reservoir are listed in the footnotes of Table 1. Hydraulic properties for the

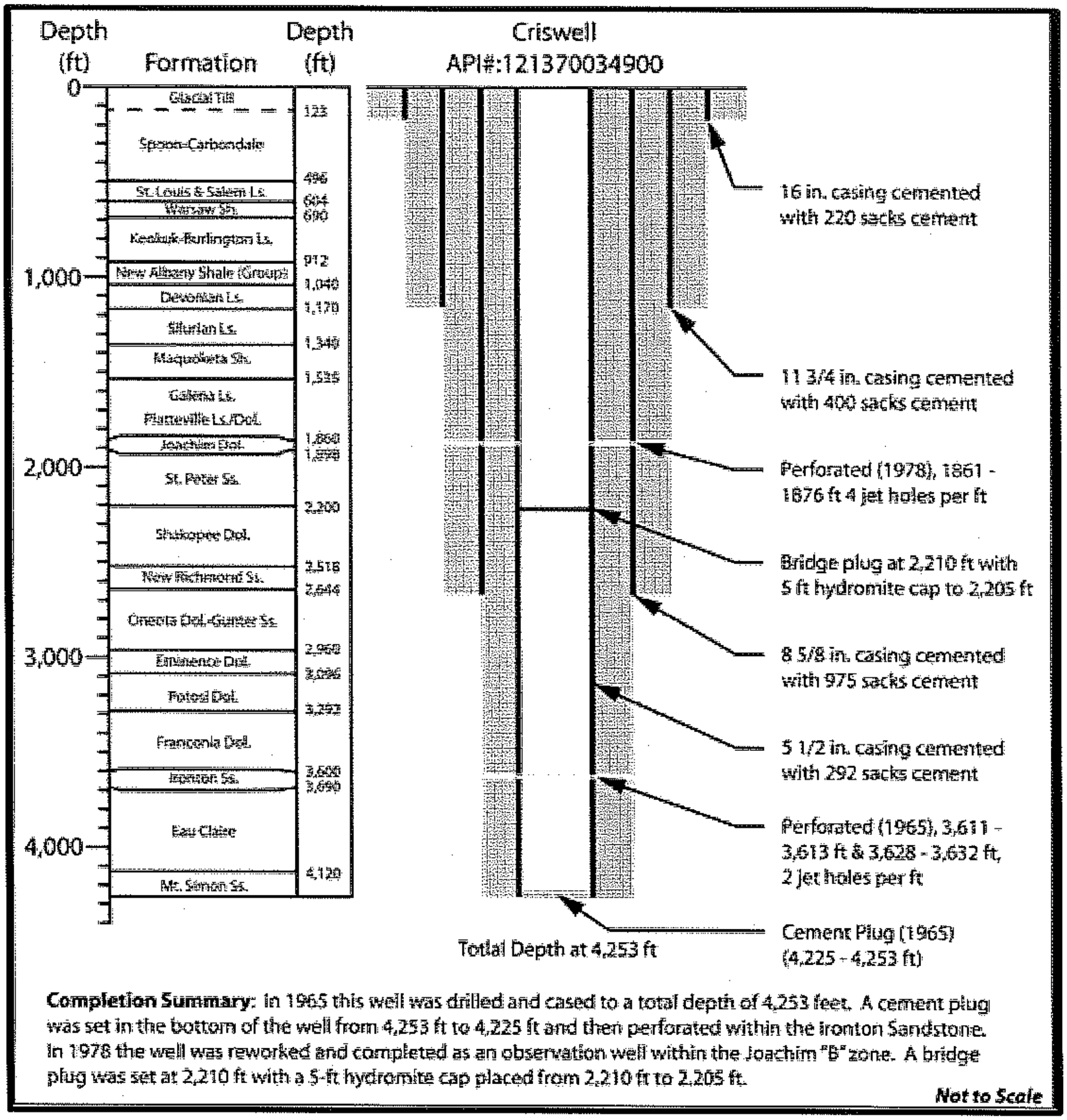

Figure 2. Diagram of the Criswell borehole at the Waverly well field (September 2012).

single-layer injection reservoir were based on fitting the simulated reservoir pressure responses from the injection model used in the UIC Permit Application at the two well locations of interest (described in more detail below).

Permeability values for the Potosi Dolomite, potentially the most permeable unit between the caprock and the lowermost USDW based on the five lost-circulation zones encountered during the initial characterization well drilling through this unit at the site, have not yet been determined for the site. Aquifer testing of this unit is planned during the next drilling campaign at the site. The Potosi Dolomite is described as a vuggy dolomite at the site and in other localities in the Illinois Basin. Preliminary estimates using a very conservative analysis based on the fluid losses during drilling indicate that the permeabilities of the lost-circulation zones are at least 5,000 mD. The permeability of the Potosi

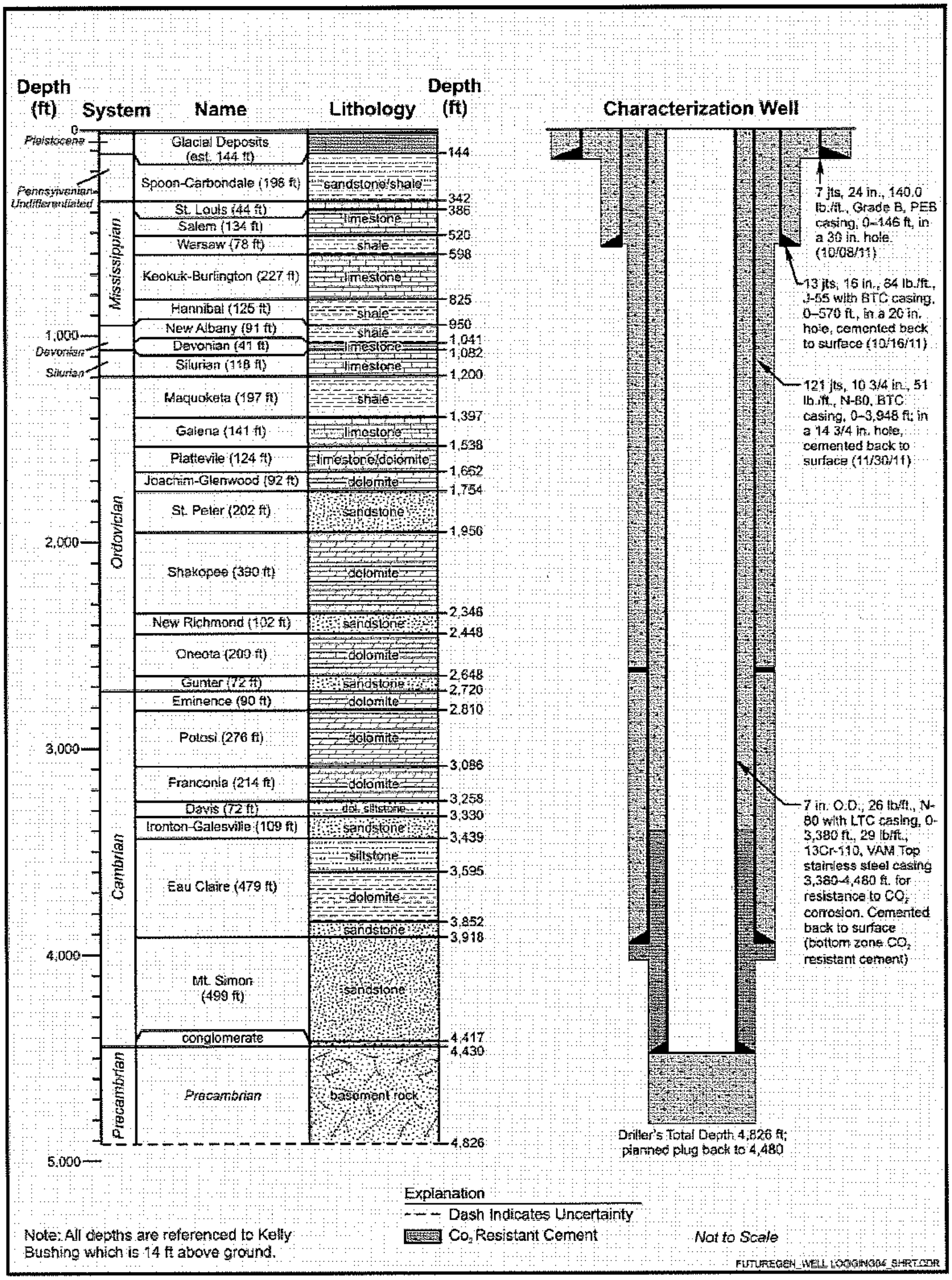

Figure 3. Diagram of FGA#1 borehole at the FutureGen 2.0 site (Figure 3.1 from PNWD-4343 [Battelle 2012]).

Dolomite at the Cabot waste injection well in Tuscola, Illinois, has been reported as 9,000 mD. Greb et al. (2009) listed permeabilities of core samples measurements for the Copper Ridge Formation, a vuggy dolomite similar to the Potosi, for a DuPont waste injection well in Louisville, Kentucky. The average horizontal permeability for the Copper Ridge Formation at the Louisville site, as reported by Greb et al. (2009), was 60 mD with the values ranging up to 632 mD. However, measurements of the permeability of core samples cannot capture the larger-scale permeability of solution cavities or fractures within this unit. The base case for this analysis uses the 9,000-mD value reported for the Tuscola site (see Table 1). Cases were also run using the much lower value of 60 mD based on the average for the Copper Ridge Formation at the Louisville, Kentucky site.

Table 1. Summary of properties used in ASLMA focused leakage model for FutureGen 2.0 site.

Unit	Thickness	Hydraulic Conductivity	Specific Storage[a]
St. Peter Sandstone	202 ft (61.6 m)	1.18E-5 m/s (1,220 mD)[b]	1.0E-6 m^{-1}
Shakopee Dolomite	390 ft (119 m)	Aquitard	Aquitard
New Richmond Sandstone	102 ft (31.1 m)	2.2E-6 m/s (230 mD)[c]	1.0E-6 m^{-1}
Oneota Dolomite, Gunter Dolomite, Eminence Dolomite	362 ft (110 m)	Aquitard	Aquitard
Potosi Dolomite	276 ft (84.1 m)	9.E-5 m/s (9,000 mD)[d]	1.0E-6 m^{-1}
Franconia Dolomite, Davis Dolomite	244 ft (74.4 m)	Aquitard	Aquitard
Ironton Sandstone	109 ft (33.2 m)	2.9E-7m/s (30 mD)[e]	1.0E-6 m^{-1}
Upper Eau Claire (Proviso and Lombard)	413 ft (126 m)	Aquitard	Aquitard
Lower Eau Clair (Elmhurst) and Upper Mount Simon	330 ft (100 m)	7.6E-7 m/s (79 mD)[f]	2.2E-6 m^{-1}[f]

(a) Specific storage for units other than reservoir: default value calculated based on mid-range of compressibility for sound rock (Table 2.5 of Freeze and Cherry [1979]). Specific storage not used for aquitards.

(b) St. Peter: Permeability from Waverly Project listed by Buschbach and Bond (1967, 1974). Measurement could be air permeability (water permeability would be lower).

(c) New Richmond: Geometric mean of a large number of samples (38) analyzed for air permeability (water permeability would be lower) from the New Richmond Formation at the Waverly site (Core Laboratories 1966).

(d) Potosi: Value reported for Potosi at Cabot Waste Injection Well in Tuscola, Illinois (see discussion in text for details).

(e) Ironton: Average of representative samples from sidewall core analyses (horizontal permeability, Klinkenberg from standard core permeability analysis and Swanson from high pressure mercury injection analysis) on samples from FGA#1 (stratigraphic characterization) borehole at the FutureGen 2.0 site (Whitney et al. 2012). Similar to geometric mean of a large number of samples (53) analyzed for air permeability from the Ironton Formation at the Waverly site (Core Laboratories 1966).

(f) Reservoir: Hydraulic properties (hydraulic conductivity and specific storage) based on fit of simulation pressure results from UIC Permit Injection model (see text for details).

Because the ASLMA model is a single-phase model, an equivalent water-injection rate was calculated from the $scCO_2$ injection rate of 1.1 MMT/yr for 20 years. The volumetric water-injection rate was calculated using $scCO_2$ densities at two pressures (see Figure 4 and Figure 5) because the UIC permit model shows a significant pressure buildup around the injection well. The first $scCO_2$ density (Figure 5) was applied for the first 5 years while injection pressures were rapidly increasing, and the second $scCO_2$ density (calculated at 400 psi higher) was applied from 5 to 20 years. The resulting water-injection rates were 0.0470 m^3/s (years 0 to 5) and 0.0439 m^3/s (years 5 to 20).

Hydraulic conductivity and specific storage were adjusted in the ASLMA model for the composite Mount Simon/Elmhurst injection layer to fit the pressure responses from the UIC permit injection model at the FGA#1 borehole (2 km from the center of the injection well laterals) and Waverly field Criswell borehole (26 km from the center of the injection well laterals). A manual fitting process was used (see comparison in Figure 6). It was difficult to exactly fit both wells with the same parameters; therefore, parameters were chosen so that the overall fit of the ASLMA pressure results for the FGA#1 and Waverly boreholes in the injection layer were mostly higher than the UIC permit model. This is conservative for this analysis because slightly greater pressures in the injection reservoir would lead to greater leakage at the well locations. The ASLMA model-predicted pressure at the injection well is much greater than the UIC permit model-predicted injection because we simulated only a single vertical well (instead of the four horizontal wells in the UIC permit model) and water injection (with a higher density and viscosity than scCO_2) with the equivalent reservoir displacement of the scCO_2. Leakage at the injection well was not part of this analysis, so this pressure difference did not affect the results (i.e., only transient pressures at the Waverly well and FGA#1 borehole were used in calculating the focused leakage into the upper units along these wells).

As shown in Figure 2.30 of the UIC Permit Application, the hydraulic heads in the Mount Simon Sandstone are higher than the St. Peter Sandstone (with differences of up to 18.8 m). We used the EPA Threshold Pressure Calculation (Equation 4 of EPA 2011) along with the pressure measurements from the St. Peter and Mount Simon from the characterization borehole (Tables 4.4 and 4.7 in Battelle 2012) to also estimate the increase in hydraulic head (above hydrostatic) to specify initial conditions for the reservoir. The hydraulic head difference from the EPA method was 25 m. For the cases run with ASLMA_V3_initialheads, the initial head for the reservoir was set to 25 m above hydrostatic pressure. The initial conditions for hydraulic heads in the aquifers above the reservoir were set to hydrostatic values.

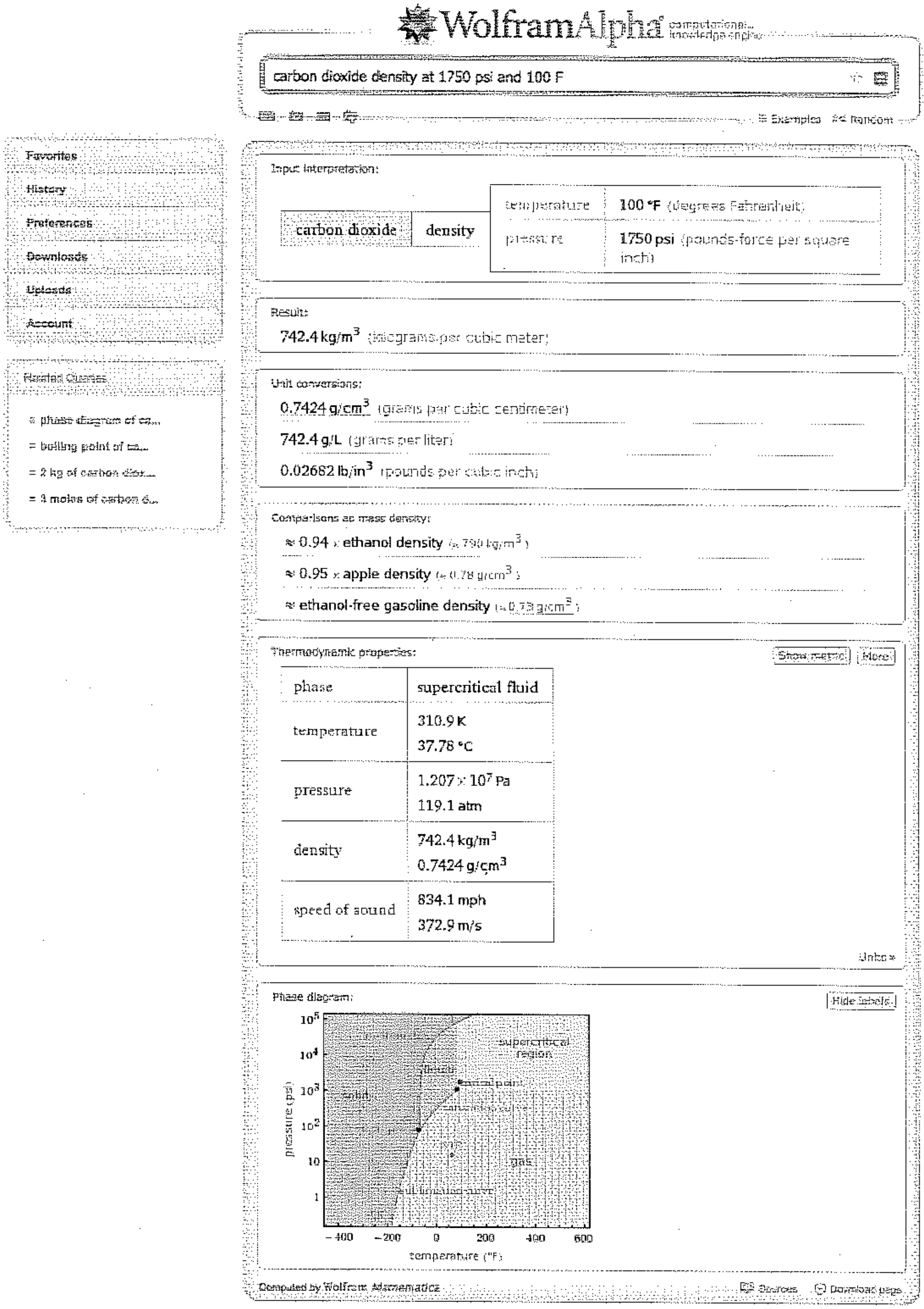

Figure 4. The $scCO_2$ density calculation for ambient conditions. (www.wolframalpha.com, accessed November 19, 2013.)

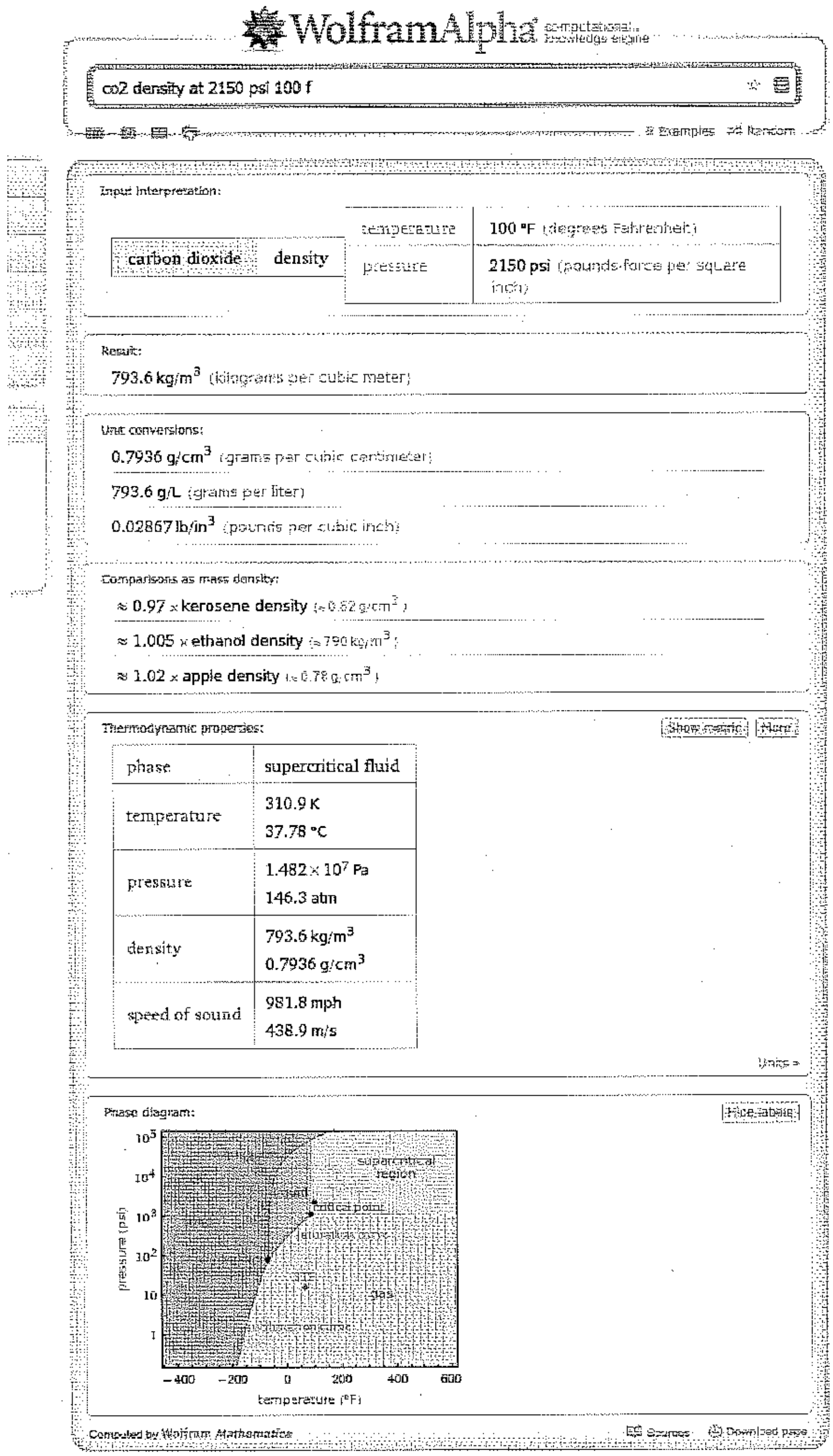

WolframAlpha computational knowledge engine

co2 density at 2150 psi 100 f

Examples Random

Input interpretation:

carbon dioxide	density	temperature	100 °F (degrees Fahrenheit)
		pressure	2150 psi (pounds-force per square inch)

Result:

793.6 kg/m³ (kilograms per cubic meter)

Unit conversions:

0.7936 g/cm³ (grams per cubic centimeter)

793.6 g/L (grams per liter)

0.02867 lb/in³ (pounds per cubic inch)

Comparisons as mass density:

≈ 0.97 × kerosene density (≈ 0.82 g/cm³)

≈ 1.005 × ethanol density (≈ 790 kg/m³)

≈ 1.02 × apple density (≈ 0.78 g/cm³)

Thermodynamic properties:

Show metric | More

phase	supercritical fluid
temperature	310.9 K 37.78 °C
pressure	1.482×10^7 Pa 146.3 atm
density	793.6 kg/m³ 0.7936 g/cm³
speed of sound	981.8 mph 438.9 m/s

Units »

Phase diagram:

Hide labels

Computed by Wolfram Mathematica

Sources | Download page

Figure 5. The $scCO_2$ density calculation for higher pressure conditions, 400 psi greater than ambient pressure. (www.wolframalpha.com, accessed November 20, 2013.)

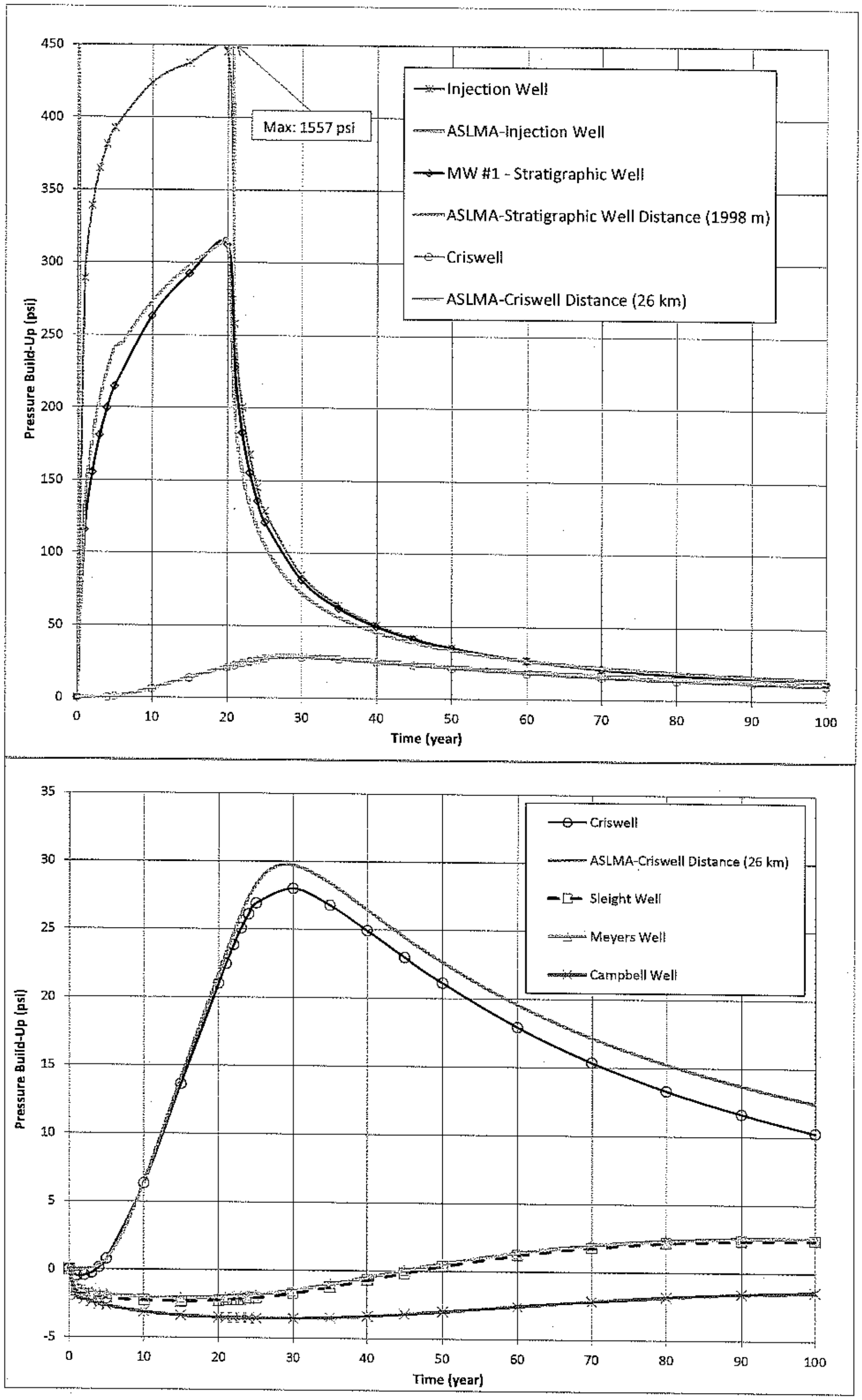

Figure 6. Comparison of pressure buildup within the Mount Simon unit between UIC Permit Model and ASLMA Model results for the FGA#1 borehole (listed as MW#1 Stratigraphic Well in plot above) and the Criswell borehole (Waverly field).

5.0 Results

Results for the simulated leakage for the Waverly field well (Criswell borehole, 26 km from the center of the injection well laterals) are shown in Figure 7 for the High Potential Leakage Category (8 mD). Figure 7 shows the total leakage from the reservoir and leakage into each of the permeable units above the caprock up to the St. Peter (lowermost USDW). The plots in Figure 7 show the fluxes over the 100-year simulation period and the cumulative leakage volume. A plot is also included, using a log scale, of cumulative leakage for the units above the Ironton (Potosi, New Richmond, and St. Peter), because these values are much lower than those for the Ironton.

Similar results for the FGA#1 borehole (at the 2-km distance) for the High Leakage Potential Category (8 mD) are shown in Figure 8. The simulated fluxes and cumulative leakage volume for the FGA#1 borehole are higher than those for the Waverly well, given the higher pressures at the closer location.

Figure 9 and Figure 10 show the simulation results for the two simulated locations (Waverly and FGA#1, respectively) using the top of the Extreme Potential Leakage Category (10,000 mD). This extreme upper bound on the effective permeability for a plugged and abandoned or poorly constructed well is comparable to unconsolidated clean sand (see Table 2.2 of Freeze and Cherry [1979]).

Table 2 shows the simulated cumulative leakage volume estimates at 100 years for each of the permeable units for comparison of the case results. Also reported in Table 2 are the results for the variations of the Extreme Potential Leakage Category cases for the two well locations. The Extreme Potential Leakage Category cases were selected because they had the highest leakage rates into the lowermost USDW. As discussed in Section 4.0, the variations include reductions in the permeability of the Potosi Dolomite (from 9,000 mD to 60 mD) along with results using the ASLMA_V3_initialheads code with the initial reservoir hydraulic heads set to 25 m higher than the hydrostatic initial conditions used in the other cases.

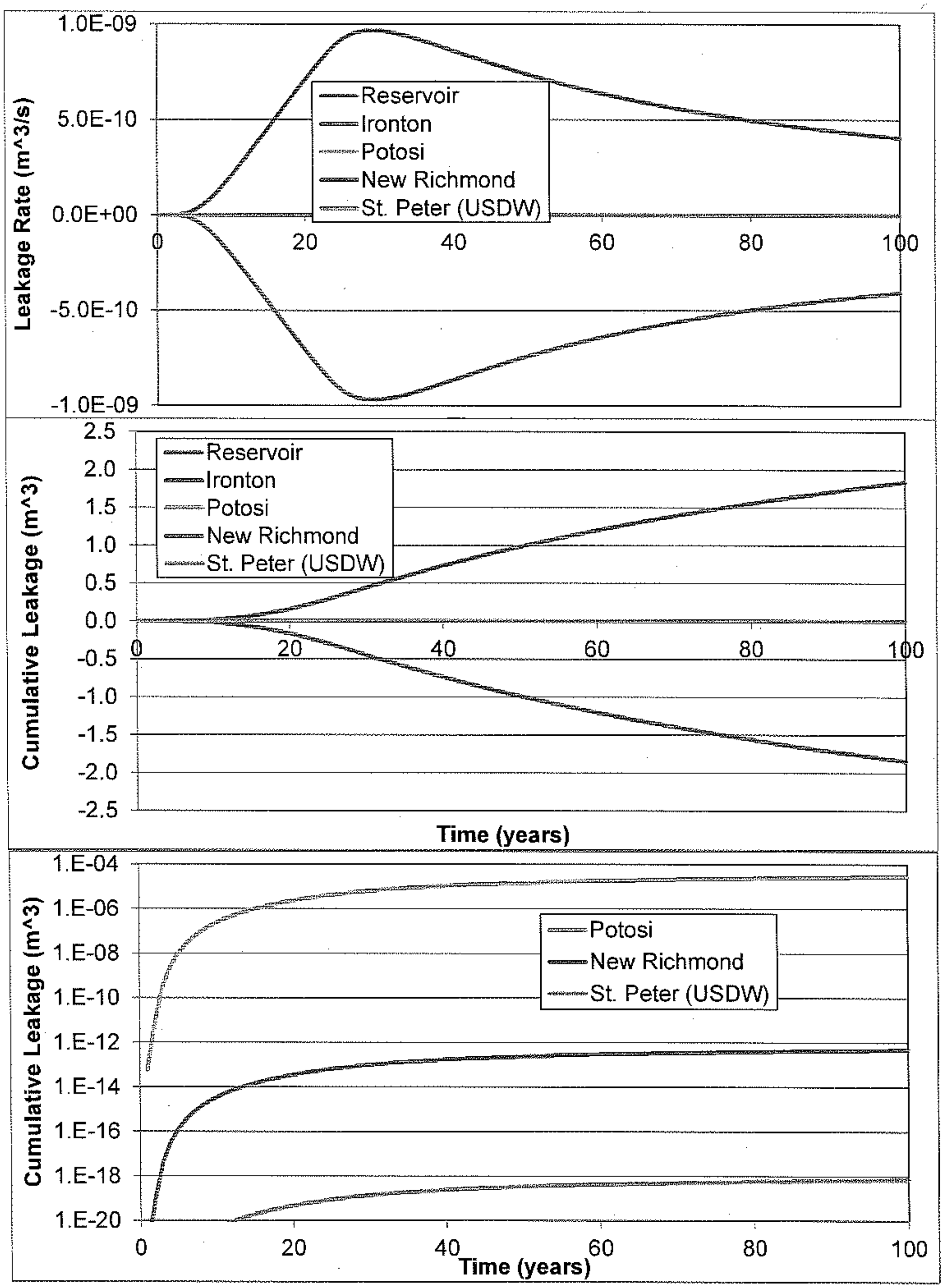

Figure 7. Waverly field well (26 km distance) – top of High Leakage Potential Category (8 mD).

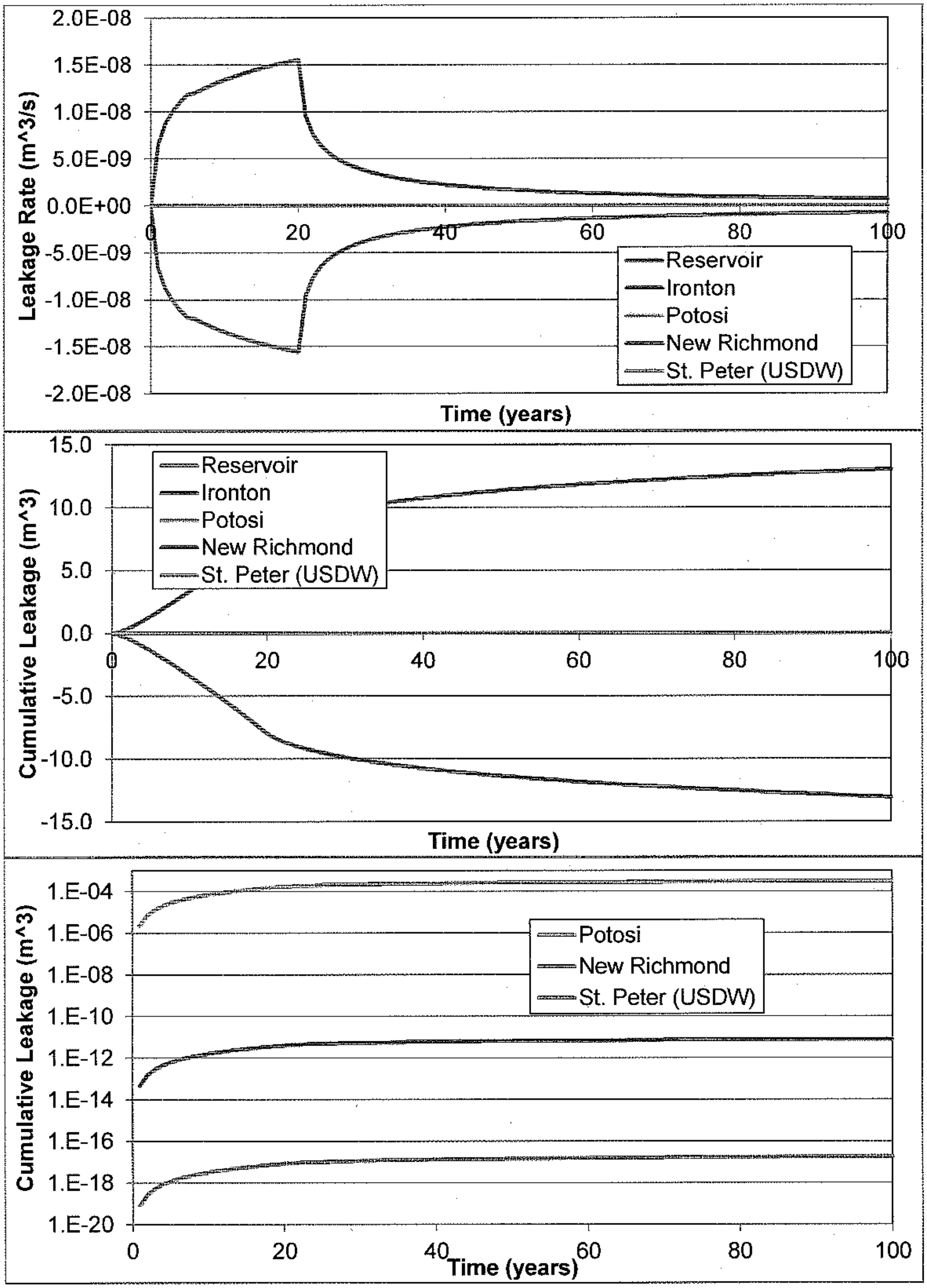

Figure 8. FGA#1 borehole (2 km distance) –top of High Leakage Potential Category (8 mD).

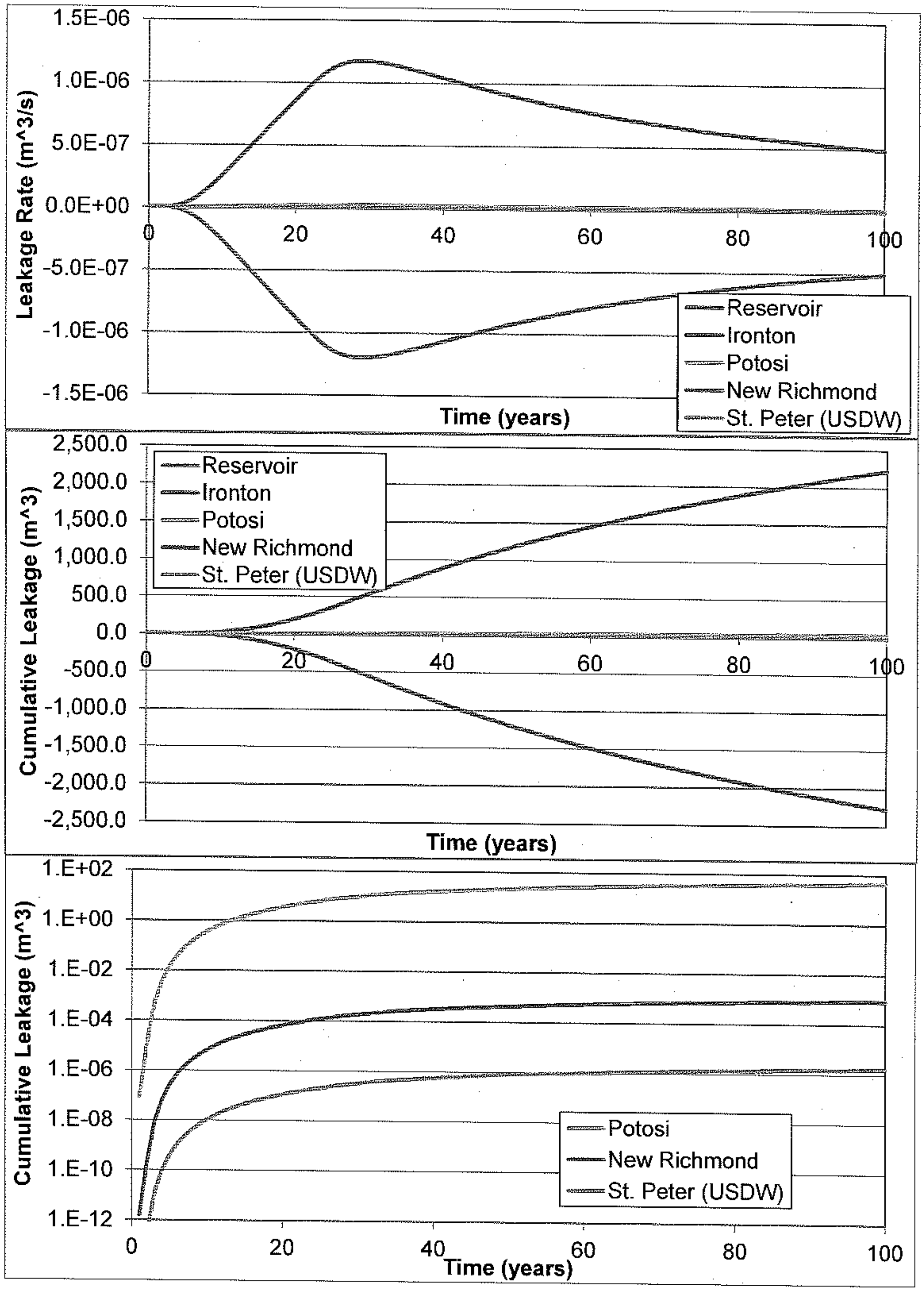

Figure 9. Waverly field well (26 km distance) – top of Extreme Leakage Potential Category (10,000 mD).

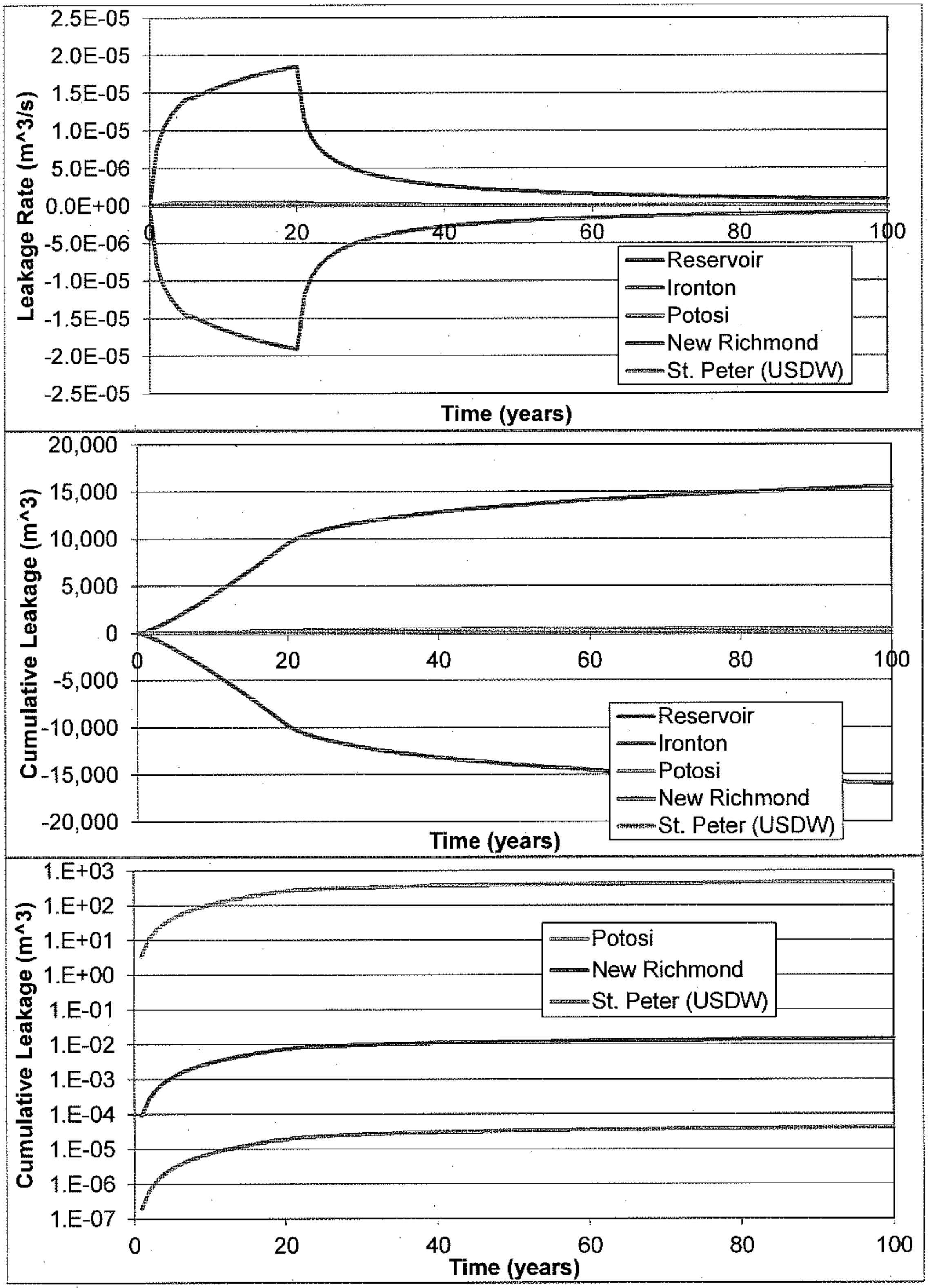

Figure 10. FGA#1 borehole (2 km distance) – top of Extreme Leakage Potential Category (10,000 mD).

Table 2. Summary of simulated cumulative fluxes after 100 years.

Case	Reservoir (Mount Simon and Elmhurst) Volume (m^3)	Ironton Sandstone Volume (m^3)	Potosi Dolomite Volume (m^3)	New Richmond Sandstone Volume (m^3)	St. Peter Sandstone Volume (m^3)
Waverly (26 km) – High Leakage Potential	-1.842	1.842	2.90E-05	4.86E-13	7.27E-19
Waverly (26 km) – Extreme Leakage Potential	-2273	2229	43.92	9.15E-04	1.71E-06
Waverly (26 km) – Extreme Leakage Potential, Lower Potosi Perm Case	-2273	2229	43.63	0.1173	2.19E-04
Waverly (26 km) – Extreme Leakage Potential, Higher Initial Heads in Mt. Simon	-1.47E+04	1.44E+04	282.2	5.85E-03	1.08E-05
FGA#1 (2 km) – High Leakage Potential	-13.04	13.04	3.13E-04	7.93E-12	1.80E-17
FGA#1 (2 km) – Extreme Leakage Potential	-1.60E+04	1.55E+04	465.1	1.47E-02	4.16E-05
FGA#1 (2 km) – Extreme Leakage Potential, Lower Potosi Perm Case	-1.60E+04	1.55E+04	460.6	1.876	5.33E-03
FGA#1 (2 km) – Extreme Leakage Potential, Higher Initial Heads in Mt. Simon	-3.46E+04	3.36E+04	991.3	3.09E-02	8.66E-05

6.0 Conclusions

Simulation results from the base cases (High and Extreme Leakage Potential) for the closest well outside of the predicted extent of the $scCO_2$ plume (Waverly field, 26 km from the center of the injection area) show that the leakage of brine into the lowermost USDW from a damaged, plugged, and abandoned or poorly constructed well, even considering extremely conservative parameter estimates, is very small. As shown in the first two rows of Table 2, a volume of only 1.71×10^{-6} m^3 (0.00171 L) or less leaks into the lowermost USDW over a period of 100 years. The simulation results show that most of the focused leakage along a damaged borehole from the reservoir is captured in the permeable zones (thief zones), most notably the Ironton Sandstone, which is the first permeable zone above the caprock (1,350 ft below the lowermost USDW [St. Peter Sandstone]). The simulated cumulative brine leakage volume from the reservoir over 100 years for the Extreme Leakage Potential Category (2,273 m^3 total or 62 L/day over this period) was mostly (i.e., 98%) into the Ironton Sandstone, as shown in Table 2. This reservoir leakage volume represents roughly 0.008% of the total $scCO_2$ injection volume (using an equivalent water-injection volume of 2.82×10^7 m^3 for 1.1 MMT/yr of $scCO_2$ based on $scCO_2$ densities discussed above over a 20-year period) for the Extreme Leakage Potential Category and much less for the High Leakage Potential Category.

Base-case simulation results for a well near the outer extent of the simulated $scCO_2$ plume (FGA#1, 2 km from the center of injection area) also resulted in very low volumes (4.16×10^{-5} m^3 [0.0416 L] or less over 100 years) of brine leakage into the lowermost USDW from a damaged, plugged, and abandoned or poorly constructed well. The Extreme Leakage Potential case at this well location did show significant leakage into the Ironton Sandstone and the Potosi Dolomite units, though both are well below the lowermost USDW. For the FGA#1 borehole, the simulated cumulative brine leakage volume from the reservoir over the 100-year period for the Extreme Leakage Potential Category (16,000 m^3 total) was also mostly (i.e., 97%) into the Ironton Formation (Table 2). This results in 2,190 L/day over a 20-year period, which is an average over a shorter time period than was used above for the Waverly well because fluxes drop off quickly after injection is over at this location. This reservoir leakage volume for the Extreme Leakage Potential Category represents roughly 0.06% of the total $scCO_2$ injection volume and a much smaller volume was predicted for the High Leakage Potential Category.

Additional cases were run with lower permeability values for the Potosi (60 mD [5 .8E-7 m/s]) based on the average listed for the Dupont Waste Injection Well in Louisville, Kentucky, for the Copper Ridge Formation, a vuggy dolomite similar to the Potosi (Greb et al. 2009). The results of these cases using the average value still showed very small amounts of leakage into the lowermost USDW over 100 years for both the Waverly field distance (0.219 L) and the FGA#1 borehole distance (5.33 L) for the Extreme Leakage Potential Category (see Table 2). Note that this lower permeability resulted in a smaller flux to the Potosi Dolomite that was partially offset by higher fluxes in the New Richmond Sandstone.

Results from the ASLMA_V3_initialheads variation runs, with the initial conditions for hydraulic heads in the reservoir set to 25 m greater than hydrostatic, are presented in Table 2 for the two well distances for the Extreme Leakage Potential Category. The cumulative leakage volumes over 100 years into the lowermost USDW are still very low for both wells (0.0108 L for Waverly and 0.0866 L for FGA#1). However, as shown in Table 2, there were large increases in the total loss from the reservoir and leakages into the Ironton Sandstone and Potosi Dolomite. It should be noted that the difference between the increased fluxes in this case compared to the base case would roughly be equivalent to the natural leakage along a damaged, plugged, and abandoned or poorly constructed well prior to any $scCO_2$ injection at the FutureGen 2.0 site (i.e., driven by ambient conditions in the area).

Results from this modeling evaluation indicated that, under site conditions, operations-related pressure increases will not result in brine migration through damaged, plugged, and abandoned or poorly constructed wells extending above overlying thief zones at appreciable levels near the outer extent of the simulated $scCO_2$ plume or at the closest well outside this zone that penetrates the caprock. Therefore, the delineated $scCO_2$ AoR should also be protective of the lowermost USDW from pressure-induced brine migration under these leakage scenarios.

7.0 References

Battelle. 2012. Borehole Completion and Characterization Summary Report for the Stratigraphic Well, Morgan County, Illinois. PNWD-4343, Battelle Pacific Northwest Division, Richland, Washington.

Birkholzer JT, JP Nicot, CM Oldenburg, Q Zhou, S Kraemer, and KW Bandilla. 2011. Brine Flow up a Borehole Caused by Pressure Perturbation from CO_2 Storage: Static and Dynamic Evaluations. *International Journal of Greenhouse Gas Control* 5(4):850-861.

Birkholzer JT, A Cihan, and KW Bandilla, and K. 2013. A Tiered Area-Of-Review Framework for Geologic Carbon Sequestration. *Greenhouse Gas Sci Technol.* doi: 10.1002/ghg.1393

Buschbach TC and DC Bond. 1967. Underground Storage of Natural Gas in Illinois – 1967. Illinois Petroleum 86. Illinois State Geological Survey, Champaign, Illinois.

Buschbach TC and DC Bond. 1974. Underground Storage of Natural Gas in Illinois – 1973 (updated). Illinois Petroleum 101. Illinois State Geological Survey, Champaign, Illinois.

Celia MA, JM Nordbotten, B Court, M Dobossy, and S Bachu. 2011. Field-scale Application of a Semi-Analytical Model for Estimation of CO_2 and Brine Leakage aong Old Wells. *International Journal of Greenhouse Gas Control* 5:257–269.

Cihan A, Q Zhou, and JT Birkholzer. 2011. Analytical solutions for pressure perturbation and fluid leakage through aquitards and wells in multilayered-aquifer systems. *Water Resour. Res.* 47.

Cihan A, JT Birkholzer, and Q Zhou. 2013. Pressure Buildup and Brine Migration During CO_2 Storage in Multilayered Aquifers. *Groundwater* 51(2).

Core Laboratories. 1966. Borehole Criswell No. 1-6 at the Waverly field: Core Laboratories, Inc. October 31, 1966, memo to Panhandle Eastern Pipeline Company, Liberal, Kansas (Waverly Field, Criswell 1-16), File #: SCAL-65269. Houston, Texas.

Crow W, JW Carey, S Gasda, B Williams, and MA Celia. 2010. Wellbore integrity analysis of a natural CO_2 producer. *International Journal of Greenhouse Gas Control* 4:186–197.

Duguid A, R Busch, JW Carey, MA Celia, N Chugunov, SE Gasda, TS Ramakrishnan, V Stamp, and JE Wang. 2013. Pre-Injection Baseline Data Collection to establish existing Well Leakage Properties. In Proceedings of the GHGT-11 Meeting, Kyoto, Japan, November 2013, *Energy Procedia.*

EPA (U.S. Environmental Protection Agency). 2011. *Draft Underground Injection Control (UIC) Program Class VI Well Area of Review Evaluation and Corrective Action Guidance for Owners and Operators*. EPA 816-D-10-007, Office of Water, Washington, D.C.

Freeze RA and JA Cherry. 1979. *Groundwater*. Published by Prentice-Hall, Inc., Englewood Cliffs, New Jersey.

Gasda SE, MA Celia, JE Wang, and A Duguid. 2013. Wellbore permeability estimates from vertical interference testing of existing wells. In Proceedings of the GHGT-11 Meeting, Kyoto, Japan, November 2013, *Energy Procedia.*

Greb SF, DC Harris, MP Solis, WH Anderson, JA Drahovzal, BC Nuttall, RA Riley, W Solano-Acosta, JA Rupp, and N Gupta. 2009. Cambrian–Ordovician Knox carbonate section as integrated reservoirs and seals for carbon sequestration in the eastern mid-continent United States. In M. Grobe, JC Pashin, and RL Dodge (eds.), Carbon dioxide sequestration in geological media—State of the science. *AAPG Studies in Geology* 59: 241–259.

Watson TL and S Bachu. 2008. Identification of Wells with High CO_2-Leakage Potential in Mature Oil Fields Developed for CO_2-Enhanced Oil Recovery. In: Paper SPE 11294, SPE Improved Oil Recovery Symposium, Tulsa, Oklahoma, USA, 19-23 April, 2008.

Whitney CL, L Parris, D Jiao, and R Lee. 2012. Core Analysis Study: FutureGen Industrial Alliance (Battelle), FutureGen #1 Well, Wildcat Field, Morgan County, Illinois. Core Laboratories Report HOU-111568, Core Laboratories, Houston, Texas.